ACS Chemical Neuroscience

pubs.acs.org/chemneuro

Research Article

Structure–Activity Assessment and In-Depth Analysis of Biased Agonism in a Set of Phenylalkylamine 5-HT$_{2A}$ Receptor Agonists

Eline Pottie,[‖] Christian B. M. Poulie,[‖] Icaro A. Simon, Kasper Harpsøe, Laura D'Andrea, Igor V. Komarov, David E. Gloriam, Anders A. Jensen, Jesper L. Kristensen,* and Christophe P. Stove*

Cite This: *ACS Chem. Neurosci.* 2023, 14, 2727–2742

Read Online

ACCESS | Metrics & More | Article Recommendations | Supporting Information

ABSTRACT: Serotonergic psychedelics are described to have activation of the serotonin 2A receptor (5-HT$_{2A}$) as their main pharmacological action. Despite their relevance, the molecular mechanisms underlying the psychedelic effects induced by certain 5-HT$_{2A}$ agonists remain elusive. One of the proposed hypotheses is the occurrence of biased agonism, defined as the preferential activation of certain signaling pathways over others. This study comparatively monitored the efficiency of a diverse panel of 4-position-substituted (and *N*-benzyl-derived) phenylalkylamines to induce recruitment of β-arrestin2 (βarr2) or miniGα_q to the 5-HT$_{2A}$, allowing us to assess structure–activity relationships and biased agonism. All test compounds exhibited agonist properties with a relatively large range of both EC$_{50}$ and E_{max} values. Interestingly, the lipophilicity of the 2C-X phenethylamines was correlated with their efficacy in both assays but yielded a stronger correlation in the miniGα_q- than in the βarr2-assay. Molecular docking suggested that accommodation of the 4-substituent of the 2C-X analogues in a hydrophobic pocket between transmembrane helices 4 and 5 of 5-HT$_{2A}$ may contribute to this differential effect. Aside from previously used standard conditions (lysergic acid diethylamide (LSD) as a reference agonist and a 2 h activation profile to assess a compound's activity), serotonin was included as a second reference agonist, and the compounds' activities were also assessed using the first 30 min of the activation profile. Under all assessed circumstances, the qualitative structure–activity relationships remained unchanged. Furthermore, the use of two reference agonists allowed for the estimation of both "benchmark bias" (relative to LSD) and "physiology bias" (relative to serotonin).

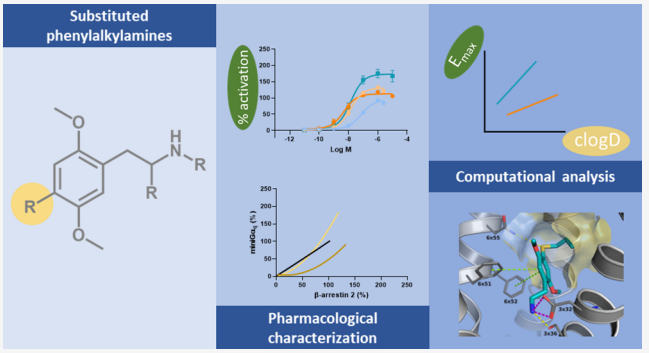

KEYWORDS: *5-HT2A, biased agonism, psychedelics, in vitro pharmacology, β-arrestin, miniGα_q*

1. INTRODUCTION

The serotonin (5-hydroxytryptamine, 5-HT) 2A receptor (5-HT$_{2A}$) is a G-protein-coupled receptor (GPCR) modulating several physiological functions, e.g., platelet aggregation and smooth muscle contraction.[1] 5-HT$_{2A}$ is also the main mediator of the psychedelic effects elicited by the serotonergic psychedelics or "classic hallucinogens,"[2−4] even though these substances typically have a complex pharmacology.[5] Overall, serotonergic psychedelics can be classified into three structural classes: ergolines, such as lysergic acid diethylamide (LSD), tryptamines exemplified by psilocin, and phenylalkylamines, with mescaline as the prototypical representative.[6] Extensive exploration of structural modifications described in PiHKAL (which is an acronym for Phenethylamines I Have Known and Loved) and TiHKAL (Tryptamines I Have Known and Loved) has resulted in an abundance of analogues.[7,8] The effects induced by serotonergic psychedelics may include mystical experiences, empathic feelings, and an altered state of consciousness, although certain substances can also lead to (severe, not necessarily 5-HT$_{2A}$-mediated) adverse events, such as headaches, agitation, convulsions, rhabdomyolysis, renal failure, and even death.[2,9,10] Recent years have witnessed a renewed therapeutic interest in psychedelics for the treatment of mood and anxiety disorders, addiction, and potentially also for the treatment of ocular hypertension, neurodegenerative disorders, and inflammation.[1,11−13]

To mediate this myriad of effects, 5-HT$_{2A}$ can couple to a variety of intracellular signal transducers that trigger distinct signaling pathways and events. The receptor primarily couples to Gα_q, and the resulting activation of phospholipase C (PLC-β) catalyzes the hydrolysis of phosphoinositides and the formation of second messengers inositol triphosphate (IP$_3$) and diacylglycerol (DAG). IP$_3$ causes the release of Ca^{2+} from

Received: April 21, 2023
Accepted: June 9, 2023
Published: July 20, 2023

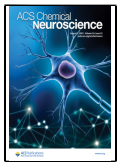

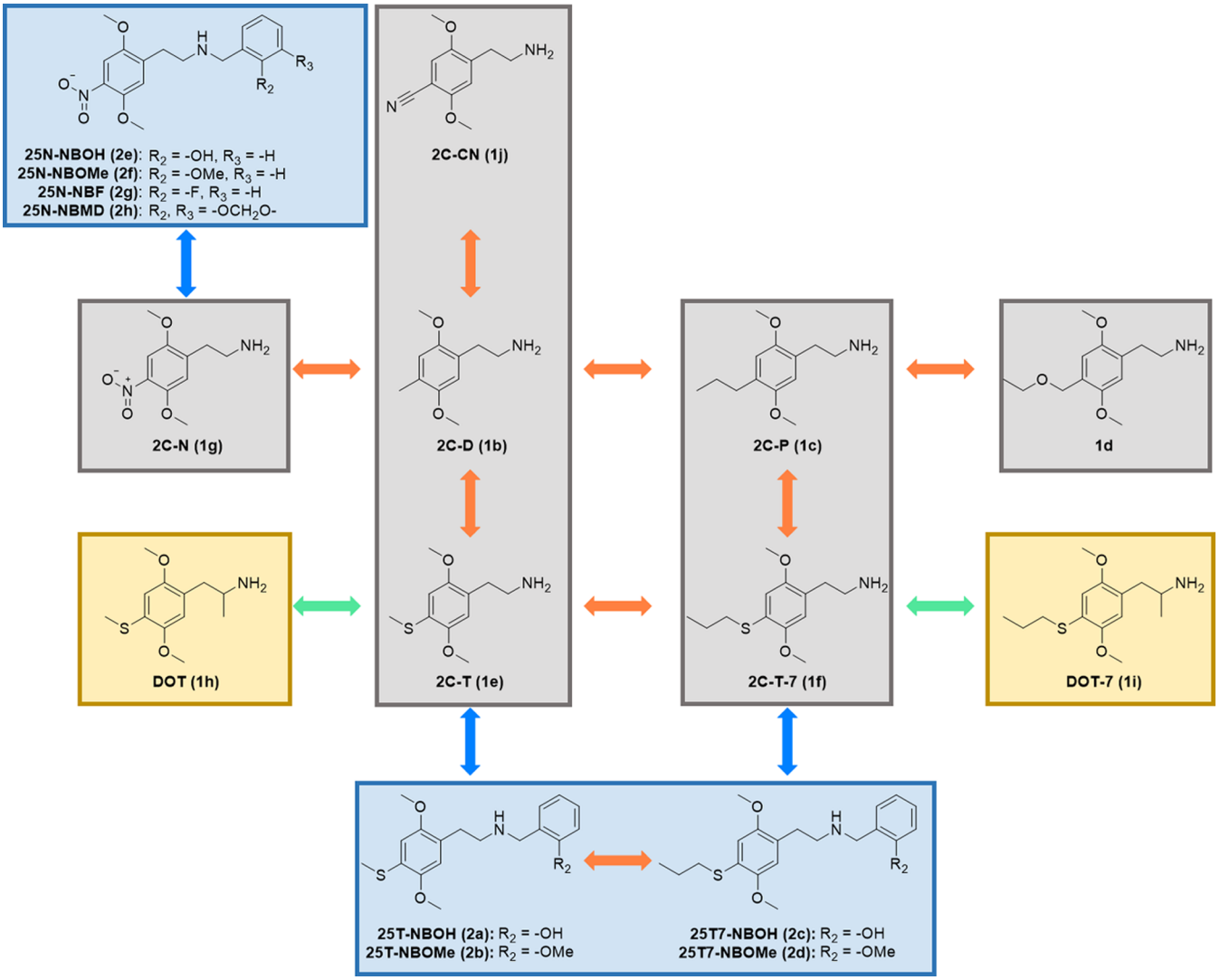

Figure 1. Schematic depiction of the structures of the phenylalkylamine analogues assessed in the present study, with phenethylamines (2C-X) highlighted in gray, phenylisopropylamines (DOX) highlighted in yellow, and *N*-benzylphenethylamines (25X-NB) highlighted in blue. Orange arrows denote the structural comparisons of compounds that only differ in terms of their 4-position substituent, green arrows indicate the comparisons of 2C-X analogues with the corresponding DOX analogues, and blue arrows indicate the comparison between 2C-X analogues and their N-benzyl-derived counterparts. The R_2 and R_3 substituents are consistent with Scheme 1.

intracellular stores, while DAG activates protein kinase C (PKC), and both events in turn stimulate distinct signaling cascades. Furthermore, 5-HT_{2A} interacts with β-arrestin (βarr), which is traditionally associated with receptor internalization and desensitization but can also mediate intracellular signaling cascades. Other responses induced by receptor activation include the interaction with ARF-1 (ADP-ribosylation factor) and the activation of effectors, such as RhoA, phospholipase D (PLD), phospholipase A_2 (PLA_2, releasing arachidonic acid (AA)), and mitogen-activated protein kinase (MAPK), inter alia.[1,4,11] Besides coupling to $G\alpha_q$, also coupling to $G\alpha_{i/o}$ proteins has been described to occur upon 5-HT_{2A} activation.[14,15]

Despite the relevance of 5-HT_{2A} agonists, the molecular and cellular mechanisms distinguishing psychedelic from non-psychedelic compounds remain elusive. In terms of receptor localization, a recent study suggests the intracellular 5-HT_{2A} to be responsible for the neuroplasticity-promoting effects of psychedelic substances.[16] One of the proposed hypotheses concerning differences in signaling properties between psychedelic and nonpsychedelic 5-HT_{2A} agonists is the signaling efficacy hypothesis, as the nonpsychedelic substance Ariadne, a structural analogue of the psychedelic DOM, showed reduced activity in different *in vitro* signaling channels.[17] Another possible explanation is the phenomenon "biased agonism," which is defined as a ligand activating one (or a subset of) signaling pathway(s) of the receptor, in preference to others.[18−22] Biased agonism is thought to arise from the stabilization of distinct active receptor conformations by different ligands/agonists,[23] and the 5-HT_{2A} receptor was actually one of the first GPCRs for which this phenomenon was proposed.[24,25] Historically, *in vitro* investigations of biased agonism at 5-HT_{2A} have compared PLC-mediated IP accumulation and PLA_2-mediated AA release.[24,26−29] More recently, βarr recruitment has been assessed comparatively to $G\alpha_q$ protein activation/recruitment.[30−32] In this context, a recent study suggested that the βarr activity of 5-HT_{2A} ligands is important for the antidepressant effects of psychedelics, while βarr recruitment alone appeared to be insufficient for the psychoactive actions, indicating that these latter effects require

https://doi.org/10.1021/acschemneuro.3c00267
ACS Chem. Neurosci. 2023, 14, 2727−2742

Table 1. Functional Properties Displayed by the Phenylalkylamine Analogues in the βarr2 and miniGα_q Recruitment Assays at the 5-HT$_{2A}$ Receptor[a]

		β-arrestin2			miniGα_q			
	$c\log D_{7.4}$	pEC_{50} (95% CI)	EC_{50} (nM) (95% CI)	E_{max} (%) (95% CI)	pEC_{50} (95% CI)	EC_{50} (nM) (95% CI)	E_{max} (%) (95% CI)	β
LSD	1.60	7.91 (7.70−8.12)	12.3 (7.56−20.0)	99.4 (92.5−106)	7.91 (7.66−8.16)	12.3 (6.99−21.8)	98.4 (90.4−107)	0
5-HT	−1.03	8.03 (7.91−8.15)	9.43 (7.16−12.4)	115 (111−119)	7.06 (6.90−7.21)	88.1 (61.4−125)	207 (196−219)	0.680
2C-CN (**1j**)	−1.27	6.76 (6.61−6.90)	174 (125−247)	73.3 (69.6−77.1)	6.30 (6.03−6.59)	503 (260−924)	85.7 (77.2−94.8)	0.412
2C-N (**1g**)	−1.13	7.49 (7.22−7.77)	32.2 (17.1−59.9)	71.5 (65.1−78.2)	7.03 (6.86−7.21)	92.5 (61.1−138)	99.7 (92.8−107)	0.305
1d	−0.91	7.58 (7.27−7.88)	26.4 (13.2−54.0)	77.5 (70.2−85.2)	7.13 (6.81−7.47)	75.0 (34.3−155)	95.8 (84.7−107)	0.323
2C-D (**1b**)	−0.65	7.79 (7.51−8.04)	16.4 (9.12−30.8)	85.7 (79.0−92.6)	7.23 (6.93−7.55)	59.4 (28.0−118)	121 (110−132)	0.372
2C-T (**1e**)	−0.52	7.88 (7.67−8.09)	13.1 (8.19−21.2)	93.9 (88.1−99.9)	7.43 (7.20−7.67)	37.1 (21.3−63.2)	121 (112−131)	0.343
2C-P (**1c**)	0.24	7.99 (7.72−8.28)	10.2 (5.31−19.3)	106 (96.5−115)	7.43 (7.17−7.70)	37.6 (20.2−68.4)	183 (167−199)	0.313
2C-T-7 (**1f**)	0.26	8.30 (8.08−8.54)	4.99 (2.90−8.30)	113 (106−120)	7.85 (7.59−8.09)	14.3 (8.12−25.5)	174 (160−188)	0.291
DOT (**1h**)	−0.28	7.84 (7.60−8.07)	14.5 (8.46−25.3)	114 (105−122)	7.18 (6.85−7.55)	65.8 (28.0−143)	191 (171−212)	0.436
DOT-7 (**1i**)	0.49	8.66 (8.35−8.96)	2.18 (1.11−4.49)	116 (107−125)	8.12 (7.78−8.48)	7.63 (3.29−16.7)	189 (169−210)	0.305
25N-NBOH (**2e**)	0.96	9.18 (8.91−9.46)	0.662 (0.35−1.23)	135 (124−147)	8.76 (8.43−9.08)	1.73 (0.825−3.72)	124 (110−137)	0.454
25T-NBOH (**2a**)	1.60	8.71 (8.48−8.94)	1.94 (1.16−3.31)	157 (146−167)	8.35 (8.10−8.62)	4.45 (2.41−7.94)	133 (123−143)	0.447
25N-NBMD (**2h**)	1.65	8.70 (8.52−8.87)	2.00 (1.35−2.99)	139 (132−146)	8.03 (7.82−8.25)	9.32 (5.68−15.1)	105 (98.1−113)	0.791
25N-NBOMe (**2f**)	1.72	8.96 (8.81−9.12)	1.09 (0.766−1.56)	173 (164−182)	8.60 (8.36−8.83)	2.53 (1.48−4.37)	168 (155−181)	0.374
25N-NBF (**2g**)	1.79	7.85 (7.70−8.00)	14.2 (10.1−20.0)	131 (125−138)	7.13 (6.96−7.30)	74.7 (49.9−110)	94.2 (87.6−101)	0.858
25T-NBOMe (**2b**)	2.29	8.69 (8.45−8.91)	2.05 (1.22−3.52)	177 (165−190)	8.37 (8.10−8.67)	4.22 (2.15−8.02)	179 (163−196)	0.332
25T7-NBOH (**2c**)	2.38	7.86 (7.70−8.02)	13.9 (9.57−20.1)	168 (157−178)	7.76 (7.47−8.04)	17.5 (9.13−34.0)	138 (124−154)	0.209
25T7-NBOMe (**2d**)	3.06	8.13 (7.91−8.35)	7.42 (4.42−12.2)	173 (160−186)	7.95 (7.64−8.26)	11.3 (5.54−23.1)	146 (130−162)	0.281

[a]Data are presented using LSD as the reference agonist and using the complete 2 h time-luminescence profile to calculate the AUC (area under the curve), from which the EC_{50} and E_{max} were derived (data analysis described in Figure S1). The EC_{50} values are measures of agonist potency of a compound in the respective assays, and the E_{max} values are measures of agonist efficacy, with the E_{max} of LSD being used for normalization. Data were combined from determinations in at least three independent experiments, each performed in duplicate. $c\log D_{7.4}$ values were calculated via Chemicalize.[43] The β-factor is the average value of the three β-factors obtained in three independent experiments.

https://doi.org/10.1021/acschemneuro.3c00267
ACS Chem. Neurosci. 2023, 14, 2727−2742

both G protein and βarr transduction. The authors propose a βarr-biased nonhallucinogenic 5-HT_{2A} agonist with antidepressant effects in mice.[33] We recently published on 25CN-NDHBF, the *N*-dihydrobenzofuran analogue of 25CN-NBOH, which showed to be a more efficacious βarr-biased agonist, but has so far only been assessed *in vitro*, with *in vivo* effects remaining elusive.[34] Kaplan et al., on the other hand, recently reported on the discovery of a $G\alpha_q$-biased nonpsychedelic 5-HT_{2A} agonist.[35]

The interpretation of ligand bias observed in *in vitro* studies is challenging due to difficulties in the translation of *in vitro* data to the *in vivo* situation, and difficulties in the interpretation of *in vitro* data per se. Among potential confounding factors related to the *in vitro* data are the temporal aspect of the readout, different expression levels of receptors and effector proteins between assays, the use of different reference agonists or highly divergent techniques, and the method of data analysis.[18,20,36,37] In the present study, we employed two highly analogous *in vitro* assay setups (miniGα_q and βarr2 recruitment to 5-HT_{2A}) in a comparative assessment of the structure−activity relationships (SARs) and the potential biased agonism exhibited by a series of phenylalkylamines. The observed differences in the pharmacological signaling were interpreted via molecular docking. The results obtained using the method we used in our previous assessments,[32,34,38] which employed LSD as a reference agonist and a continuous 2 h activation profile for the calculation of EC_{50} and E_{max}, were compared here to using serotonin as a reference agonist and applying a different time point (the first 30 min of the continuous activation profile) for data calculation. The assessment of two reference agonists allowed for the estimation of two types of biased agonism: benchmark bias relative to LSD, and physiology bias relative to serotonin. Qualitative and quantitative methods were used to evaluate these different types of bias.

2. RESULTS AND DISCUSSION

2.1. Structure−Activity Relationships of the Ligands in Two Analogous Bioassays. A panel of diversely substituted phenylalkylamines (Figure 1) was synthesized and chemically characterized according to the procedures described in Section 3. The compounds comprise phenethylamines (2C-X, depicted in gray frames in the figure), phenylisopropylamines (DOX, in yellow frames), and *N*-benzylphenethylamine (25X-NB, in blue frames) derivatives. All compounds were tested in parallel in βarr2- and miniGα_q-(the engineered GTPase domain of the $G\alpha_q$ subunit)[39] recruitment assays employing the Nanoluciferase Binary Technology (NanoBiT) system. As our previous data obtained via these assays have been published using the prototypic psychedelic drug LSD as the reference agonist and employing the entire 2 h time-luminescence profile for the calculation of the AUC,[32,34,38,40−42] in Table 1 we present the results in those same conditions.

Our functional data show that LSD (used as reference agonist in Table 1) and serotonin displayed similar EC_{50} and E_{max} values in the βarr2 recruitment assay (12.3 nM and 99.4% vs 9.43 nM and 115%, respectively). In the miniGα_q recruitment assay, however, the potency of LSD was ∼7-fold higher than that of serotonin (EC_{50} values of 12.3 and 88.1 nM, respectively), while the determined E_{max} for LSD was only half of that observed for serotonin (98.4 and 207%, respectively). This trend, as well as the obtained EC_{50} and E_{max} values, is in agreement with our earlier findings, employing the same experimental setup.[34,38] Using a stable cell line expressing the components of the βarr2 recruitment assay rather than transiently transfected cells, as employed here, we have previously determined agonist potency and efficacy values for 2C-T-7 (**1f**) and 2C-D (**1b**), and the data for these two compounds were in line with the values obtained here.[41]

The results allowed us to estimate the effect caused by the introduction of an α-methyl group (DOX) and the addition of a substituted *N*-benzyl moiety (25X-NB) to 2C-X substances (Figure 1, green and blue arrows, respectively). DOT (**1h**, or Aleph), the α-methyl derivative of 2C-T (**1e**) displayed comparable agonist potencies to 2C-T (**1e**) but increased agonist efficacies [E_{max}: 114% (βarr2), 191% (miniGα_q)]. These are remarkably high values for a DOX analogue, but this observation agrees with previously described patterns from phenylisopropylamine and phenethylamine comparisons, which showed that the addition of an α-methyl group to the 2C-X scaffold, yielding the DOX analogues, results in similar potencies but increased efficacies.[28,41,44] DOT-7 (**1i**, or Aleph-7), the phenylisopropylamine (DOX) analogue of 2C-T-7, displayed a divergent activity profile from the "typical" pattern described above. Particularly, 2C-T-7 (**1f**) and DOT-7 (**1i**) had comparable potencies and efficacies in both assays, with particularly high efficacies in the miniGα_q recruitment assay for both substances.

The addition of an *ortho*-substituted benzyl group at the amine of 2C-T (**1e**) yielded 25T-NBOH (**2a**) and 25T-NBOMe (**2b**), leading to a marked increase in potency and efficacy in the two assays, compared to the parent phenethylamine 2C-T (**1e**). The only exception was the efficacy of 25T-NBOH (**2a**) in the miniGα_q assay, which was similar to that of 2C-T (**1e**). Employing βarr2 and miniGα_q recruitment assays, as well as a PI hydrolysis assay, it has been reported that the introduction of an *N*-benzyl function yields agonist analogues with higher potencies and efficacies than their 2C-X counterparts.[32,41,45] However, others have reported similar potencies and decreased efficacies for the NB-derived analogues, compared to the 2C-X counterparts, in a FLIPR assay.[46] Likewise, the two *N*-benzyl substituted derivatives of 2C-T-7 (**1f**), 25T7-NBOH (**2c**) and 25T7-NBOMe (**2d**), also displayed a divergent pattern. The potency of 25T7-NBOH (**2c**) in the βarr2 recruitment assay was reduced compared to 2C-T-7 (**1f**), while its efficacy was markedly higher than that of the parent compound. On the other hand, while the potencies of 2C-T-7 (**1f**) and 25T7-NBOH (**2c**) were comparable in the miniGα_q recruitment assay, 25T7-NBOH (**2c**) exhibited a lower efficacy in this assay. For 2C-T-7 (**1f**) and 25T7-NBOMe (**2d**), the agonist potencies were very similar in both assays, with the introduction of the *N*-benzyl substitution increasing agonist efficacy in the βarr2 assay and slightly decreasing the efficacy in the miniGα_q assay (Table 1).

Various *N*-benzyl substitutions of 2C-N yielded analogues with the following agonist potency ranking: 2C-N (**1g**) < 25N-NBF (**2g**) < 25N-NBMD (**2h**) < 25N-NBOMe (**2f**) < 25N-NBOH (**2e**) in both assays (Table 1). 25N-NBOH (**2e**) was found to possess a remarkably high potency, exhibiting a sub-nanomolar EC_{50} value in the βarr2 recruitment assay (Table 1), thus rendering it the most potent analogue in this study. In both assays, 25N-NBOMe (**2f**) was the nitro analogue with the highest agonist efficacy. The remarkably high potency observed for most of the 25N compounds was consistent with

https://doi.org/10.1021/acschemneuro.3c00267
ACS Chem. Neurosci. 2023, 14, 2727−2742

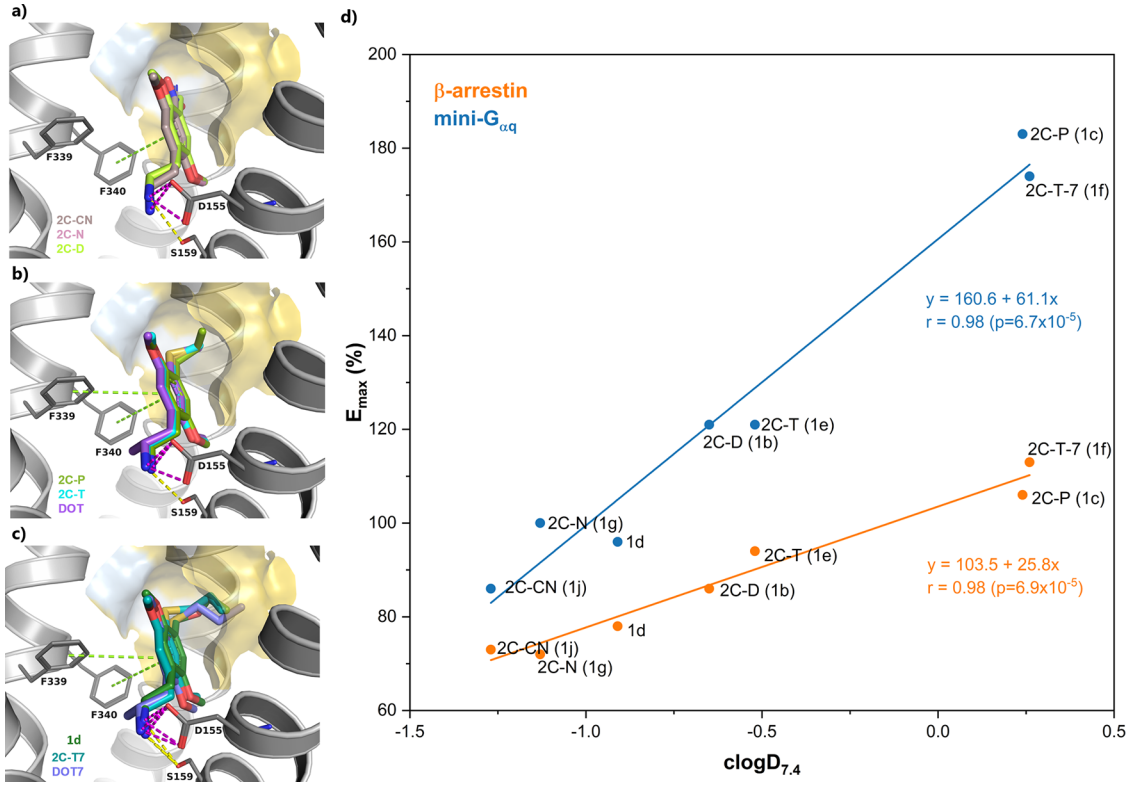

Figure 2. (a–c) Predicted binding poses and ligand–receptor interactions of selected 4-substituted phenethylamines at the 5-HT_{2A}. The ligands are displayed as sticks, while the receptor is shown as gray lines and cartoon. Ligand–receptor interactions are displayed as dashed lines and colored in green (aromatic, $\pi-\pi$ stacking), yellow (hydrogen bond), and pink (salt-bridge). The receptor hydrophobic sub-pocket between TM4 and TM5 is shown as a surface and colored according to the Eisenberg hydrophobicity scale,[58] from highly hydrophilic (blue) to highly hydrophobic (yellow). (d) Linear correlation curve between the miniGα_q (blue) and βarr2 (orange) recruitment assay E_{max} values and calculated *c* log *D* values at pH 7.40.

observations by Eshleman et al., who reported a sub-nanomolar EC_{50} for 25N-NBOMe (**2f**) in a PI hydrolysis assay.[47] All efficacies obtained for the *N*-benzyl substituted analogues were higher than those of 2C-N in both assays, except for 25N-NBF (**2g**) in the miniGα_q recruitment assay. The low activity of 25N-NBF concords with previous findings of 25X-NB derivatives with other 4-position substituents.[32,41,48]

In the literature, the *in vitro* structure–activity relationship (SAR) of 2C-X, DOX, and *N*-benzyl derivatives has been assessed via different methods.[28,41,44−46,49,50] Apparent discrepancies between the results reported here and the literature could be explained by differences in experimental conditions, as *in vitro* assay outcomes can be influenced by the specific assay platform, the choice of reference agonist, the assay temperature—which can influence ligand kinetics—the serum starving of cells, the expression levels of receptor and effector/transducer proteins and their potential adaptations (such as the introduction of a tag), and the compound's stability in these conditions, among other things. Furthermore, distinct readouts may yield different results, e.g., endpoint readout vs a continuous readout, and the time point chosen for analysis. Importantly, the selection of an *in vitro* assay inherently always entails both advantages and limitations. For a more detailed analysis of factors potentially contributing to an assay's outcome, the reader is referred to Pottie and Stove.[37]

In the case of serotoninergic receptors, serotonin, which is naturally present in serum, can affect receptor expression levels or lead to agonist-induced receptor internalization.[37] This is relevant, as this can potentially affect an assay's readout. We therefore evaluated whether our results would be different using serum-starved cells or using cells grown in medium containing dialyzed serum. Experimental procedures are outlined in the Supporting Information. In this assay format, serum starving the cells did not appear to influence receptor surface expression levels, as shown in Figure S2. Furthermore, also growing the cells in dialyzed serum, which does not contain serotonin, did not yield results different from those with the described culturing conditions (Figure S3 and Table S1).

Aside from the comparison of the activities between 2C-X, DOX, and 25X-NB substances with the same 4-substituent (Figure 1, green and blue arrows), the data allowed us to assess the structure–activity relationship of differently substituted 2C-X substances (Figure 1, orange arrows). The seven 2,5-dimethoxy-phenethylamines (Figure 1, highlighted in gray) are substituted with 4-cyano, 4-nitro, 4-alkylthio, 4-alkyl, or 4-ethoxymethyl groups. 2C-CN (**1j**), which has a cyano group at the *para*-position of the phenyl ring displayed an EC_{50} value of 174 nM and an E_{max} of 73.3% in the βarr2 recruitment assay, and an EC_{50} value of 503 nM and an E_{max} of 85.7% in the miniGα_q recruitment assay (Table 1). The 2C-X analogue with a slightly less hydrophilic nitro group, 2C-N (**1g**), displayed substantially lower EC_{50} values (32.2 and 92.5 nM in the βarr2 and miniGα_q recruitment assays, respectively) and similar E_{max} values (71.5 and 99.7%, respectively). Interestingly, we observed that increasing the lipophilicity of the 2C-X substances (estimated by the calculated octanol/water

https://doi.org/10.1021/acschemneuro.3c00267
ACS Chem. Neurosci. 2023, 14, 2727−2742

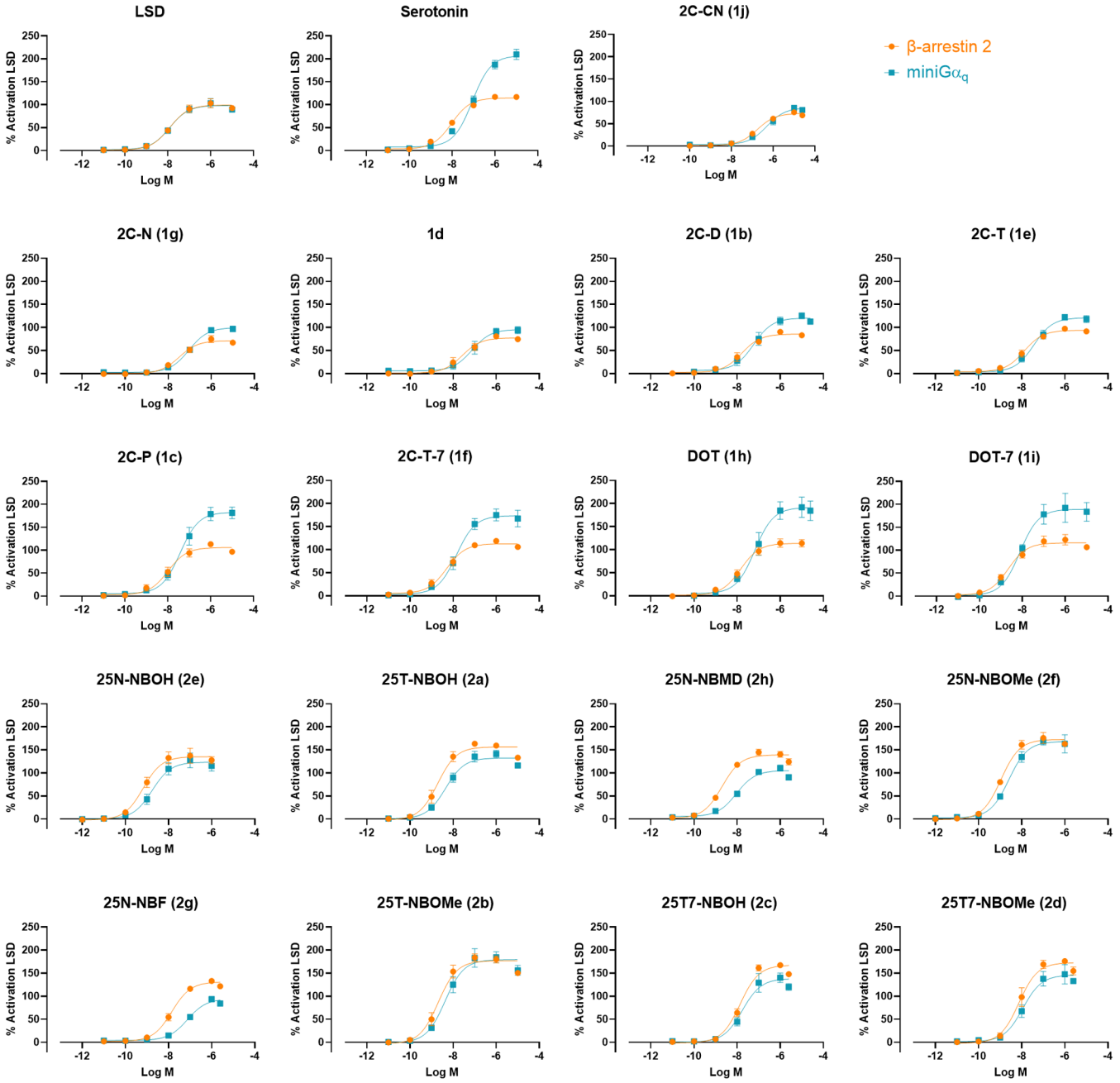

Figure 3. Concentration−response curves for each of the compounds in the βarr2 (orange) and miniGα_q (blue) recruitment assays at the 5-HT$_{2A}$. Each point represents the mean of three independent experiments, each performed in duplicate ± SEM (standard error of the mean). Curves represent three parametric, nonlinear fits of normalized and pooled data for each concentration tested, normalized with LSD as a reference agonist.

distribution at pH 7.4 ($c\log D_{7.4}$ values in Table 1)) coincided with an increase in the potency and efficacy in both assay formats, with low nanomolar EC_{50} values and extraordinarily high E_{max} values (up to 174−183%, relative to LSD) for 2C-T-7 and 2C-P in the miniGα_q assay.

2.1.1. Computational Interpretation of the Results in the 2C-X Group. Since the only variable group within the subset of 2C-X compounds is in the 4-position of the phenethylamine, the differences in their $c\log D_{7.4}$ values solely reflect the contribution of that moiety to the overall ligand lipophilicity. Interestingly, we found a strong linear correlation ($r = 0.98$, $p < 0.0001$) between ligand lipophilicity and the agonist efficacies displayed by these compounds in both assays (Figure 2d). The slope of the curves, however, differed considerably, being twice as high for the miniGα_q (61.1) as for the βarr2 (25.8) assay. These observations suggested that an increase in the ligand lipophilicity favored receptor activation and increased the recruitment of both effector proteins, but that the miniGα_q-mediated recruitment was more significantly impacted. Although these results aligned with previous reports that 5-HT$_{2A}$ ligand affinity and activity increases with ligand lipophilicity,[51−53] to the best of our knowledge, this is the first report indicating that lipophilicity may favor the recruitment of one signaling protein (miniGα_q) over another (βarr2). Importantly, we cannot rule out that (some of the) observed effects can (partially) be explained by the presence of -and action at- intracellular 5-HT$_{2A}$. Indeed, it can be anticipated that with increasing lipophilicity the potential of

https://doi.org/10.1021/acschemneuro.3c00267
ACS Chem. Neurosci. 2023, 14, 2727−2742

compounds to penetrate the cell membrane will also increase. In this context, recent research elegantly demonstrated the importance of intracellular 5-HT_{2A} in the effect of membrane-permeable substances, but not of membrane-impermeable substances, such as serotonin.[16] Irrespective of the 5-HT_{2A} fraction(s) responsible for the observed effects, the differences observed between both recruitment assays remain interesting. While the evaluation of (differential) signaling by cell surface and intracellular 5-HT_{2A} fractions is a fascinating future research avenue, it was beyond the scope of this manuscript to further investigate this additional layer of complexity.

In an attempt to rationalize our experimental observations, we docked the ligands in the cryo-EM structure of 5-HT_{2A} bound to 25CN-NBOH and coupled to a miniGα_q chimera (PDB 6WHA).[54] As a means of validation of the protocol, the docked position of 25CN-NBOH is shown in Figure S4 and compared to the experimentally determined binding mode, displaying an RMSD of 0.57 Å for all ligand heavy atoms. All phenethylamines displayed similar top ranking binding modes (Figure 2), with similar interactions to those of 25CN-NBOH (Figure S4), which included (i) a salt-bridge interaction between the positively charged amine and Asp155^{3x32}—a key interaction for ligands targeting aminergic GPCRs;[55] (ii) hydrogen bonding interaction between the positive amine and Ser159^{3x36}; and (iii) aromatic (π-π) interactions between the phenethylamine ring and residues Phe339^{6x51} and Phe340^{6x52}.[56] These two phenylalanine residues are strictly conserved in the serotonergic GPCR family, being responsible for the binding of serotonin's indole ring[57] and playing a critical role in 2C-X/DOX binding and receptor activation at the 5-HT_{2A}.[45] Our docking results suggested that the various 4-substituents in the phenethylamine ring occupied a subregion of the binding pocket between TM4 and TM5 (Figure 2). This sub-pocket is primarily formed by hydrophobic residues and is capable of hosting 4-substituents as large as methoxyethyl, propyl, and propylthio (Figure 2a–c). Moreover, due to its hydrophobic nature, interaction with this pocket apparently improves with increasing 4-substituent lipophilicity. This is further supported by the estimated distances between the terminal heavy atom of the 4-substituent in the predicted binding pose of the phenethylamine substances and the closest side chain heavy atom of the residues lining this hydrophobic pocket between TM4 and TM5 in the 5-HT_{2A} receptor, as shown in Figure S5.

We hypothesize that the interaction between the 4-substituent of the 2C-X series and the hydrophobic pocket results in a conformational change at the 5-HT_{2A} which differentially impacts the recruitment of miniGα_q and βarr2. Thus, the interaction of 2C-X ligands containing longer (and more hydrophobic) 4-alkyl or -alkylthio chains, such as 2C-P (**1c**) and 2C-T-7 (**1f**), with this hydrophobic sub-pocket promotes more efficacious miniGα_q- than βarr2-recruitment, compared to ligands such as 2C-D (**1b**) and 2C-T (**1e**), which possess shorter 4-alkyl or -alkylthio chains, and even more when compared to 2C-CN (**1j**) and 2C-N (**1g**), containing comparatively more hydrophilic 4-substituents (Figure 2). It is tempting to conclude that hydrophobic ligand moieties located in this sub-pocket between TM4 and TM5 could be utilized to design ligands with preference for miniGα_q over βarr2 recruitment. However, even though the limited variation of 4-substituents investigated for DOX and *N*-benzyl-derived substances does not make a similar analysis possible, it appears that the same correlation between E_{max} and lipophilicity of 4-substituents did not hold true for the DOX and *N*-benzyl-substituted analogues (Table 1). Apparently, there is an (additional) interplay with the substituent pattern on or near the protonated nitrogen, which may favor different receptor conformations. Future in-depth analysis of distinctly substituted analogues may yield additional valuable insights on the effect of the 4-substituent.

2.2. Estimation of the Level of Biased Agonism. Aside from assessing the structure–activity relationships of the test compounds, the use of the two assay formats allowed for the estimation of biased agonism, which is typically a complex matter. In an attempt to counter the complexity associated with bias estimates and their interpretation, community guidelines on experiment design and reporting have now been published by the International Union of Pharmacology.[18] One important consideration is the definition of the system in which the biased agonism is characterized, with the notion that results obtained in one system may not necessarily be translatable to others. Importantly, while the two NanoBiT recruitment assays described in this study allow us to estimate biased agonism at the upstream level in two highly similar assays, this does not allow us to discern how a differential recruitment of effector proteins translates into distinct outcomes further downstream.

In this study, different quantitative and qualitative measures assessing biased agonism have been employed to interpret the obtained results. For the data obtained with LSD as a reference agonist and using the AUC of the 2 h time–response curves for data calculation, these measures are shown in Figure 3 (the averaged concentration–response curves for each analogue in the two functional assays), Figure 4 (quantitative bias factors, calculated with LSD as a reference agonist), Figure 5 (bias plots, each plotting curves for LSD as the reference agonist and one of the tested compounds), and Figure 6 (the rank orders of the agonist efficacies displayed by the compounds in the two assays). Although overlaid curves (Figure 3), not encompassing data obtained for a reference agonist, are not strictly a means to identify biased agonism, they do allow us to rapidly capture diverging functional properties.

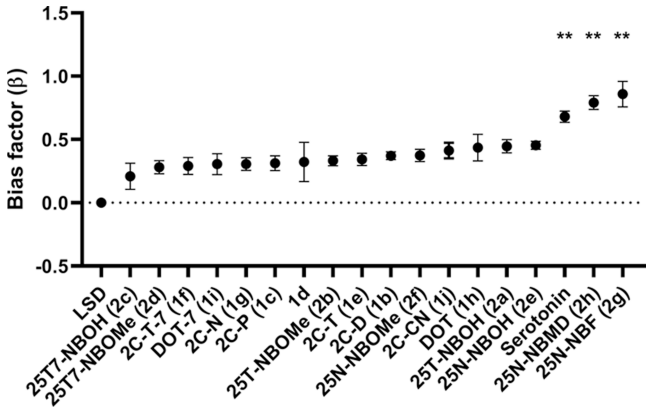

Figure 4. Visual representation of the bias factors (β) ± SEM (standard error of the mean), where ** stands for $p < 0.01$ in the nonparametric Kruskal–Wallis analysis of significance with post hoc Dunn's test. LSD is used as the reference agonist.

In Figure 4, the calculated bias factors (β) are plotted. From the formula, it can be derived that a bias factor close to 0 entails no strongly distinguishable difference from the signaling pattern of the reference agonist LSD in the two measured

https://doi.org/10.1021/acschemneuro.3c00267
ACS Chem. Neurosci. 2023, 14, 2727–2742

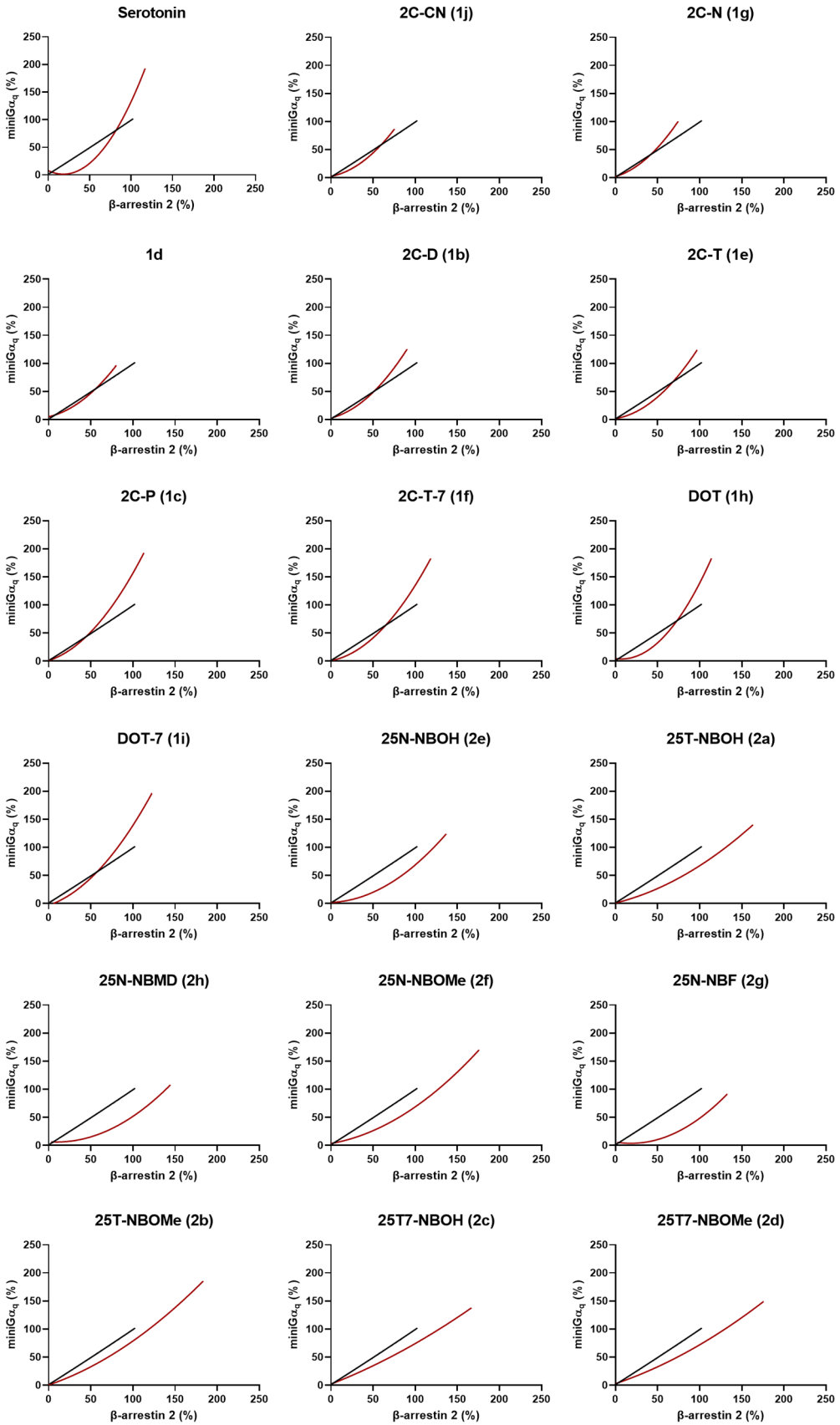

Figure 5. Qualitative bias plots, where each panel shows the centered second-order polynomial fit of the activation values at equimolar concentrations of the substance in the respective assays in red, and that of the reference agonist (in this case LSD) in black.

https://doi.org/10.1021/acschemneuro.3c00267
ACS Chem. Neurosci. 2023, 14, 2727−2742

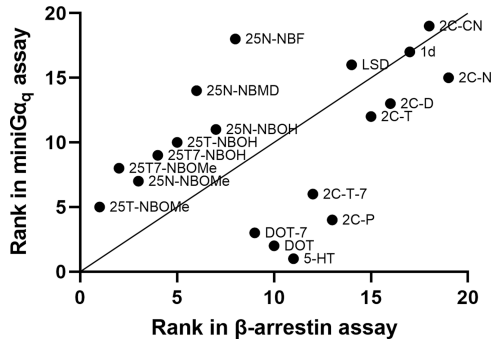

Figure 6. Visual representation of the differences in ranking order of the substances' efficacies in the βarr2 and miniGα_q assay at the 5-HT$_{2A}$. The *x*-axis shows the relative ranking of the substance in the βarr2 assay, and the *y*-axis shows that in the miniGα_q assay. The substances that are on the right part of the "identity line" have a relative preference toward miniGα_q recruitment, and the ones above the line toward βarr2 recruitment, with substances being further away from the unity line having a larger difference in ranking order.

outcomes, while a positive value suggests a relative preference toward βarr2 recruitment, and a negative value a preferential recruitment of miniGα_q, relative to LSD. In this set of compounds, all bias factors had positive values and statistical analysis revealed the bias factors of 25N-NBF (**2g**), 25N-NBMD (**2h**), and the endogenous agonist serotonin to be statistically significantly different from LSD (Figure 4). While these positive values nicely reflected the higher efficacy and more potent activities of 25N-NBMD (**2h**) and 25N-NBF (**2g**) in the βarr2 assay than in the miniGα_q assay, they did not account for the markedly higher efficacies of e.g., serotonin, 2C-T-7 (**1f**), DOT-7 (**1i**), DOT (**1h**), 2C-P (**1c**), and 2C-D (**1b**) in the miniGα_q assay. From our previous study, using the same experimental setup, it also emerged that this quantitative measure has its limitations and might not always reflect the qualitative interpretation.[32] Furthermore, a study extensively comparing different methods of bias calculation unraveled discrepancies between bias assessed by widely used methods.[20]

In recent guidelines, the use of bias plots has been suggested to nonquantitatively confirm the existence of bias between two assays.[18,23,59] The qualitative interpretation emerging from the plots in Figure 5 indicated a clear preference toward βarr2 over miniGα_q recruitment for all 25X-NB substances relative to LSD. For the other tested compounds, the identification of a preference toward either recruitment assay is less straightforward since their curves cross that of the reference agonist. This indicates, in theory, that at lower concentrations the agonist preferentially induces recruitment of one intracellular protein, switching preference at higher concentrations.

Another proposed solution to avoid using models for ligand bias assessment is to compare the rank order of the agonist efficacies among the competing assays.[20] In Figure 6, the ranks of agonist efficacies of the test compounds in the βarr2 (*x*-axis) and miniGα_q (*y*-axis) recruitment assays are plotted. When the identity line is drawn, the substances that are closer to the *x*-axis are more inclined toward miniGα_q recruitment, while those closer to the *y*-axis are more inclined toward βarr2 recruitment. Moreover, the further from the identity line, the larger the differences in rank order between the two assays. In this approach, the classification of a given compound will depend on the character of the other substances in the same panel. In this case, 25N-NBF (**2g**) and 25N-NBMD (**2h**) again stand out as the compounds with the strongest preference toward βarr2 (relative to LSD), with the other 25X-NB substances lying above the identity line, while serotonin, DOT (**1h**), DOT-7 (**1i**), 2C-P (**1c**), and 2C-T-7 (**1f**) have a relatively stronger preference toward miniGα_q recruitment. These findings appear to contradict the calculated bias factors, which indicated a strong preference of serotonin toward βarr2 recruitment. Again, this illustrates the challenge of unequivocal interpretation of biased agonism in a given dataset. Looking into the comparison of the different methods, it is not surprising that different methods can yield different results, as distinct factors are taken into consideration by each method. For example, the quantitative bias factors (Figure 4 and Table 1) take into account both E_{max} and EC$_{50}$, whereas the "ranking method" (Figure 6) only considers the eventual E_{max} of each compound (e.g., explaining the above-mentioned apparent discrepancy for serotonin). The bias plot, on the other hand, also reflects the course of the concentration−response curve, as also seen in the overlaid concentration−response curves.

From Figure 6, the overlaid curves (Figure 3), and the bias plots (Figure 5), it can be deduced that the 2C-X substances display either "unbiased" profiles compared to LSD or show a relative preference toward miniGα_q recruitment, especially at higher concentrations. Moreover, the fact that 2C-P (**1c**) and 2C-T-7 (**1f**) are the 2C-X analogues that lie furthest away from the identity line indicates their preference toward recruitment of miniGα_q. This is also reflected in our computational finding that, with increasing lipophilicity of a substance, the efficacy of miniGα_q recruitment increases comparatively more than that of βarr2 recruitment. All *N*-benzyl-derived substances, on the other hand, lie above the identity line, an indication of their preference toward the recruitment of βarr2 over miniGα_q recruitment, compared to LSD. This preference is also reflected in the bias plots (Figure 5), and the overlaid curves (Figure 3). 25N-NBF (**2g**) and 25N-NBMD (**2h**), which lie the furthest above the identity line, additionally have bias factors that are statistically significantly different from LSD, with a clear preference toward βarr2. The relative βarr2-preferring character of these *N*-benzyl (particularly -NBMD and -NBF) derivatives is consistent with our observations in a previous study.[32] However, further investigation of these substances is required to draw definitive conclusions.

2.3. Estimation of Structure−Activity Relations and Relative Bias Is Not Influenced by Time Point of Calculation. The time point at which the pharmacological parameters and bias estimates are calculated can affect the interpretation of functional assays' results.[18,36] Therefore, in addition to using the 2 h AUC to generate concentration−response curves, the potency and efficacy values were also extracted from the time-luminescence profiles using the AUC values from the first 30 min (Table S2 and Figures S6−S8). Comparison of Table 1 with Table S2 shows that the obtained EC$_{50}$ values for the 30 min profiles in both assays were consistently slightly higher, although with overlapping confidence intervals (with only four exceptions). For the βarr2 recruitment assay, the E_{max} values were similar in the two measurement situations, whereas the E_{max} values in the miniGα_q assay were consistently higher for the 30 min profiles, even though confidence intervals were overlapping for all compounds except serotonin. Despite these numerical differences, the qualitative interpretation did not diverge from that outlined above, except for the comparison between LSD and serotonin in the βarr2 recruitment assay, as the EC$_{50}$ value of

https://doi.org/10.1021/acschemneuro.3c00267
ACS Chem. Neurosci. 2023, 14, 2727−2742

LSD was higher than that of serotonin when using the first 30 min of the activation profile, as also observed in a previous study.[38]

From the calculated bias factors, the same compounds as described above emerged as statistically significantly biased toward the recruitment of βarr2, relative to LSD: 25N-NBMD, 25N-NBF, and serotonin. These results show that taking a different time point for calculating the obtained data does not yield a divergent interpretation of the results, but results in rather small numeric differences. However, it cannot be excluded that other time points and/or other ligands would yield different effects. Significant differences between assays have been found when assessing different time points. Wacker et al. reported on a substantial increase in the potency of LSD upon increasing incubation times, tested in various assay formats, but each format having an endpoint readout, which may lead to different relative data interpretations.[30]

2.4. Influence of the Employed Reference Agonist on the Observed Outcomes. Reference agonists allow the comparison of results across studies by reducing system biases that depend on system properties, such as the experimental setup and the cell line used. As both the reference agonist and the tested ligands are influenced by the same confounders in a similar way, the use of a reference agonist cancels out (or at least reduces) the effects of these factors when comparing across different systems.[18,21] The well-described psychedelic LSD and the endogenous 5-HT_{2A} agonist serotonin are frequently used references in the literature. Therefore, we included serotonin as a second reference agonist in this set of experiments (Table S3 and Figures S9−S11). Comparing the data in Table 1 with those in Table S3, it is clear that the obtained EC_{50} values differ only marginally and show overlapping confidence intervals (the differences can actually be explained by rounding differences in the calculation of normalized values). A schematic overview of the data analysis is provided in Figure S1. On the other hand, the relative E_{max} values change more profoundly, especially for the miniGα_q assay, resulting in a more narrow range of efficacies. This is not surprising given the similar E_{max} values displayed by LSD and serotonin in the βarr2 assay and the 2-fold higher E_{max} of serotonin compared to LSD in the miniGα_q assay. More importantly, the use of a different reference agonist did not markedly influence the observed relative structure−activity relationships. Additionally, the data in Table S4 show that the use of the first 30 min of the activation profile with serotonin as a reference agonist did not alter the previous conclusions about structure−activity relationships, despite numerical differences.

However, the choice of the reference agonist did affect the bias determination. In the preceding sections, LSD was used as the reference agonist because of its high relevance in the context of psychedelic substances and for comparability with previous studies.[18,32,38,40−42] Inherently, the resulting outcomes are solely a measure of biased agonism relative to LSD in the respective systems (i.e., "benchmark bias"), without inferring pathway-biased agonism, where bias estimates are relative to an established "balanced" reference agonist, or physiology-biased agonism, where bias estimates are relative to the endogenous agonist, representing signaling in the physiological situation—it should be noted that an endogenous agonist is not necessarily "balanced."[18] As serotonin, used as a second reference ligand, is also the endogenous agonist of the 5-HT_{2A}, physiology-biased agonism is being assessed when using serotonin as the reference comparator. The pharmacological parameters and bias estimates with serotonin as reference are provided in Table S3 and Figures S9−S11.

From Figure S10, it can be derived that the quantitative bias factors follow the same trend as those in Figure 4. However, all values are ∼0.7 lower than those obtained with LSD as a reference agonist, hence yielding negative values for all substances (indicative of a preference toward the recruitment of miniGα_q compared to serotonin), except for 25N-NBMD (**2h**) and 25N-NBF (**2g**). The most negative value is that of LSD. Again, these calculated bias factors do not necessarily support the qualitative observations in the overlaid curves (Figure S9), where many of the substances yield higher and more leftward-shifted curves (indicative of a higher potency) for the recruitment of βarr2 compared to miniGα_q. The estimation of bias from the bias plots (Figure S11) yielded clear preferences toward the recruitment of βarr2 over miniGα_q recruitment relative to serotonin for certain substances, e.g., 25N-NBMD (**2h**) and 25N-NBF (**2g**). On the other hand, the plots of 2C-D (**1b**), 2C-P (**1c**), **1d**, 2C-T-7 (**1f**), DOT-7 (**1i**), 2C-T (**1e**), 2C-N (**1g**) and DOT (**1h**) suggested a (slight) relative preference toward the recruitment of miniGα_q. Measures of biased agonism using the first 30 min of the activation profile largely yielded similar observations (Table S4 and Figures S12−S14).

In conclusion, we reported here on a comparative analysis of a set of 2C-X, DOX, and *N*-benzyl-derived phenylalkylamine analogues with differing lipophilic characters in two highly analogous recruitment assays at the 5-HT_{2A}. In both assays, EC_{50} values and E_{max} values spanned a broad range, and the obtained values enabled SAR assessment. The analysis revealed that the E_{max} values of the 2C-X analogues in both assays correlated to the calculated *c* log $D_{7.4}$ values, a measure of their lipophilicity. A molecular docking approach supported the hypothesis that this effect may be related to the positioning of the 4-substituent of 2C-X substances in a highly hydrophobic pocket between TM4 and TM5 of 5-HT_{2A}. Further analysis is warranted to confirm the observed pattern over a broader range of 2C-X substances and to verify whether such pattern also exists for the DOX and *N*-benzyl-derived phenylethylamines. Furthermore, the concomitant use of two assays allowed for the assessment of biased agonism, hinting at 2C-X substances being either unbiased or (weakly) miniGα_q-preferring compared to LSD and the *N*-benzyl-derived analogues showing a relative preference toward βarr2 recruitment, when assessing the outcomes via qualitative methods. However, these qualitative findings are not necessarily reflected in the quantitative bias factors, except for 25N-NBF (**2g**) and 25N-NBMD (**2h**), which show the strongest preference toward βarr2 recruitment when using LSD as reference agonist. The use of the endogenous 5-HT_{2A} agonist serotonin as an alternative reference agonist, or calculation of the outcomes at a different time point, did not affect the interpretation of the SAR, although the obtained numerical values obviously differed. Furthermore, the use of two reference agonists also enabled the estimation of both "benchmark"- and "physiology"-based bias. Although clearly different outcomes were obtained, depending on the reference used, the relative trends of the bias factors remained, irrespective of the reference. Altogether, this study has provided novel insights into the structure−activity relationships of a set of diversely substituted phenylalkylamines and has utilized the data obtained from two highly related *in vitro*

https://doi.org/10.1021/acschemneuro.3c00267
ACS Chem. Neurosci. 2023, 14, 2727−2742

assays to perform an in-depth analysis of the concept of biased agonism at 5-HT_{2A}.

3. MATERIALS AND METHODS

3.1. Chemicals and Reagents. Dulbecco's modified Eagle's medium (DMEM), OptiMEM, amphotericin B, penicillin/streptomycin, and Hank's Balanced Salt Solution (HBSS) were purchased from Fisher Scientific (Merelbeke, Belgium). FuGENE HD transfection reagent and NanoGlo Live Cell Reagent were from Promega (Madison, WI). Serotonin and poly-D-lysine hydrobromide were bought from Sigma-Aldrich (Steinheim, Germany), and the analytical standards of LSD (lysergic acid diethylamide) and 25D-NBOMe HCl from were purchased from Chiron AS (Trondheim, Norway).

3.2. Chemical Synthesis of the Test Compounds. The phenethylamine analogues were all prepared according to previously described methods.[7,48,60] Briefly, the corresponding aldehyde was condensed with nitromethane or nitroethane and the resulting nitrostyrene was subsequently reduced with lithium aluminum hydride. **1d** was prepared via formylation of the 4-position of phthalimide-protected 2,5-dimethoxyphenethylamine followed by reduction and alkylation with ethyl iodide, and final deprotection with hydrazine.[60] 2C-N (**1g**) was prepared from 2,5-dimethoxyphenethylamine (**1a**), via nitration of the 4-position.[7] In order to obtain phenethylamine 2C-CN (**1j**), compound **1a** was brominated in the *para*-position and subsequently the amine was converted to the corresponding phthalimide.[7] This was followed by a copper-catalyzed cyanation on the 4-bromo moiety and subsequently the amine was deprotected with NH_2NH_2.[61] The *N*-benzyl analogues were prepared via reductive amination of the corresponding phenethylamines and the appropriate benzylaldehyde. 25T-NBOH, 25T-NBOMe, 25T7-NBOH, and 25T7-NBOMe (**2a−2d**, respectively) were prepared according to the previously reported method.[48] 25N-NBOH, 25N-NBOMe, 25N-NBF, and 25N-NBMD, (**2e−2h**, respectively) were prepared in a similar fashion starting from 2C-N (**1g**), in ∼70% yield (Scheme 1).

All reactions involving dry solvents or sensitive agents were performed under a nitrogen atmosphere and glassware was dried prior to use. Commercially available chemicals were used without further purification. Solvents were dried prior to use with an SG water solvent purification system or dried by standard procedures, and reactions were monitored by analytical thin-layer chromatography (TLC, Merck silica gel 60 F_{254} aluminum sheets). Flash chromatography was carried out using Merck silica gel 60A (35−70 μm). ^{1}H NMR spectra were recorded on a 400 MHz Bruker Avance III or 600 MHz Bruker Avance III HD, and ^{13}C NMR spectra on a 101 MHz Bruker Avance III or 151 MHz Bruker Avance III HD. Analytical HPLC was performed using an UltiMate HPLC system consisting of an LPG-3400A pump (1 mL/min), a WPS-3000SL autosampler, and a 3000 Diode Array Detector installed with a Gemini-NX C18 (250 × 4.60 mm^2, 3 μm) column. Solvent A: H_2O + 0.1% TFA; Solvent B: MeCN-H_2O 9:1 + 0.1% TFA. For HPLC control, data collection, and data handling, Chromeleon software v. 6.80 was used. UHPLC-MS spectra were recorded using an Acquity UPLC H-Class Waters series solvent delivery system equipped with an autoinjector coupled to an Acquity QDa and TUV detectors installed with an Acquity UPLC BEH C18 (50 × 2.1 mm^2, 1.7 μm) column. Solvent A: 5% aq. MeCN + 0.1% HCO_2H: Solvent B: MeCN + 0.1% HCO_2H. Usually, gradients from A:B 1:0 to 1:1 (5 min) or A:B 1:0 to 0−50 (5 min), were performed depending on the polarity of the compounds. For data collection and data handling, MassLynx software was used. Compounds were dried under high vacuum or freeze-dried using a ScanVac Cool Safe Freeze Drier. The purity of compounds submitted for pharmacological characterization was determined by ^{1}H NMR and HPLC to be >95%.

3.2.1. General Procedure (A) for the Synthesis of Secondary Amines. The aldehyde (1.1 equiv) was added to a suspension of the phenethylamine hydrochloride (1 equiv) and Et_3N (1.0 equiv) in EtOH. The reaction mixture was stirred until the formation of the imine was complete (30 min to 3 h). After addition of $NaBH_4$ (2.0 equiv), the mixture was stirred for 45 min and concentrated under reduced pressure. The residue was partitioned in CH_2Cl_2/H_2O (1:1 v/v) and the aqueous phase was further extracted with CH_2Cl_2 (2×). The organic layers were combined, dried over $NaSO_4$, filtered, and evaporated under reduced pressure. The secondary amine product was purified by column chromatography (CH_2Cl_2/MeOH + Et_3N, 98.2:1.4 + 0.25%) and precipitated by the addition of HCl in dioxane (1.5 equiv) under continuous stirring. The solid fraction was filtered, dried under reduced pressure, dissolved in a minimum amount of MeOH, and precipitated by the addition of Et_2O. The product was collected by filtration and dried under reduced pressure.

*3.2.1.1. 2-(2,5-Dimethoxy-4-methylphenyl)ethan-1-amine Hydrochloride (2C-D, **1b**).* **1b** was prepared according to reported conditions.[7,48] Characterization was in accordance with reported values.

*3.2.1.2. 2-(2,5-Dimethoxy-4-propylphenyl)ethan-1-amine Hydrochloride (2C-P, **1c**).* **1c** was prepared according to reported conditions.[7,48] Characterization was in accordance with reported values.

*3.2.1.3. 2-(4-(Ethoxymethyl)-2,5-dimethoxyphenyl)ethan-1-amine Hydrochloride (**1d**).* **1d** was prepared according to reported conditions, and the characterization was in accordance with reported values.[60]

*3.2.1.4. 2-(2,5-Dimethoxy-4-(methylthio)phenyl)ethan-1-amine Hydrochloride (2C-T, **1e**).* **1e** was prepared according to reported conditions.[7,48] Characterization was in accordance with reported values.

*3.2.1.5. 2-(2,5-Dimethoxy-4-(propylthio)phenyl)ethan-1-amine Hydrochloride (2C-T-7, **1f**).* **1f** was prepared according to reported conditions.[7,48] Characterization was in accordance with reported values.

*3.2.1.6. 2-(2,5-Dimethoxy-4-nitrophenyl)ethan-1-amine Hydrochloride (2C-N, **1g**).* **1g** was prepared according to reported conditions.[7] ^{1}H NMR (600 MHz, DMSO) δ 7.98 (br, 3H), 7.51 (s, 1H), 3.89 (s, 3H), 3.83 (s, 3H), 3.04 (t, J = 7.1 Hz, 2H), 2.94 (t, J = 7.3 Hz, 2H). ^{13}C NMR (151 MHz, DMSO) δ 150.4, 146.1, 137.7, 132.5, 116.8, 107.2, 57.0, 56.3, 38.0, 27.9.

*3.2.1.7. 1-(2,5-Dimethoxy-4-(methylthio)phenyl)propan-2-amine Hydrochloride (DOT, **1h**).* **1h** was prepared according to reported conditions.[7,62] Characterization was in accordance with reported values. ^{1}H NMR (600 MHz, DMSO) δ 7.96 (s, 3H), 6.82 (s, 1H), 6.76 (s, 1H), 3.79 (s, 3H), 3.76 (s, 3H), 3.42−3.35 (m, 1H), 2.87 (dd, J = 13.3, 5.9 Hz, 1H), 2.70 (dd, J = 13.3, 8.2 Hz, 1H), 2.41 (s,

Scheme 1. Synthesis of the Phenylalkylamines and Their Corresponding *N*-Benzyl Analogues[a]

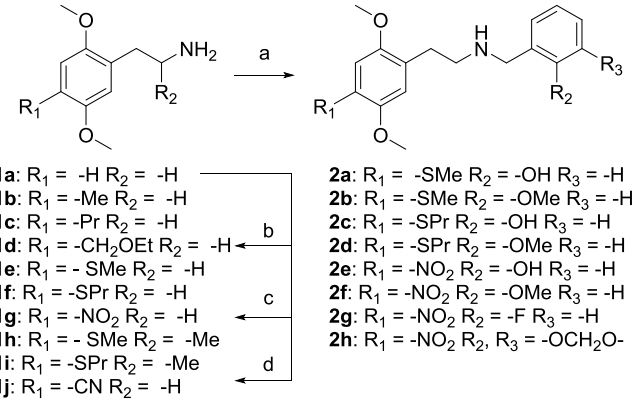

[a]Reaction conditions: (a) (i) aldehyde, EtOH, rt; (ii) $NaBH_4$, EtOH, rt; (b) (i) phthalic anhydride, toluene, reflux; (ii) $TiCl_4$, dichloromethyl methyl ether/4-chlorobutanoyl chloride, CH_2Cl_2, −10 to 0 °C; (iii) $NaBH_4$, EtOH, rt; (iv) NaH, EtI, DMF, 0 °C to rt; (v) hydrazine (aq.), THF, rt; (c) HNO_3 (70%), AcOH, 0 °C−rt. (d) (i) Br_2, AcOH, rt; (ii) phthalic anhydride, toluene, reflux; (iii) Cu(I)CN, DMF, reflux; (iv) hydrazine (aq.), THF, rt.

https://doi.org/10.1021/acschemneuro.3c00267
ACS Chem. Neurosci. 2023, 14, 2727−2742

3H), 1.11 (d, J = 6.6 Hz, 3H). ^{13}C NMR (151 MHz, DMSO) δ 151.8, 149.4, 125.9, 121.1, 113.9, 109.1, 56.2, 56.1, 46.9, 34.6, 17.9, 13.7.

*3.2.1.8. 1-(2,5-Dimethoxy-4-(propylthio)phenyl)propan-2-amine Hydrochloride (DOT-7, **1i**).* **1i** was prepared according to reported conditions.[7,62] Characterization was in accordance with reported values. ^{1}H NMR (600 MHz, DMSO) δ 7.94 (s, 3H), 6.83 (s, 1H), 6.83 (s, 1H), 3.77 (s, 3H), 3.76 (s, 3H), 3.43−3.35 (m, 1H), 2.92−2.83 (m, 3H), 2.70 (dd, J = 13.3, 8.1 Hz, 1H), 1.59 (h, J = 7.3 Hz, 2H), 1.11 (d, J = 6.5 Hz, 3H), 0.99 (t, J = 7.3 Hz, 3H). ^{13}C NMR (151 MHz, DMSO) δ 151.5, 150.3, 123.9, 122.1, 114.3, 111.2, 56.2, 56.0, 46.9, 34.6, 32.6, 21.7, 17.9, 13.3.

*3.2.1.9. 2-(((2,5-Dimethoxy-4-(methylthio)phenethyl)amino)-methyl)phenol Hydrochloride (25T-NBOH, **2a**).* **2a** was prepared according to reported conditions, and the characterization was in accordance with reported values.[48]

*3.2.1.10. 2-(2,5-Dimethoxy-4-(methylthio)phenyl)-N-(2-methoxybenzyl)ethan-1-amine Hydrochloride (25T-NBOMe, **2b**).* **2b** was prepared according to reported conditions, and the characterization was in accordance with reported values.[48]

*3.2.1.11. 2-(((2,5-Dimethoxy-4-(propylthio)phenethyl)amino)-methyl)phenol Hydrochloride (25T7-NBOH, **2c**).* **2c** was prepared according to reported conditions, and the characterization was in accordance with reported values.[48]

*3.2.1.12. 2-(2,5-Dimethoxy-4-(propylthio)phenyl)-N-(2-methoxybenzyl)ethan-1-amine Hydrochloride (25T7-NBOMe, **2d**).* **2d** was prepared according to reported conditions, and the characterization was in accordance with reported values.[48]

*3.2.1.13. 2-(((2,5-Dimethoxy-4-nitrophenethyl)amino)methyl)-phenol Hydrochloride (25N-NBOH, **2e**).* Synthesized from 2-(2,5-dimethoxy-4-nitrophenyl)ethan-1-amine hydrochloride and salicylaldehyde by general procedure A in 72% yield as an orange solid. ^{1}H NMR (600 MHz, DMSO) δ 7.45 (s, 1H), 7.21 (s, 1H), 7.05 (d, J = 7.1 Hz, 2H), 6.70 (dt, J = 2.0, 7.4 Hz, 1H), 6.67 (q, J = 3.3 Hz, 1H), 3.87 (s, 3H), 3.81 (s, 2H), 3.78 (s, 3H), 2.81 (t, J = 3.0 Hz, 2H), 2.78 (t, J = 2.9 Hz, 2H). ^{13}C NMR (151 MHz, DMSO) δ 157.2, 150.3, 146.3, 136.9, 136.0, 128.5, 127.8, 124.2, 118.4, 116.5, 115.3, 107.1, 56.1, 54.9, 50.3, 47.6, 30.0.

*3.2.1.14. 2-(2,5-Dimethoxy-4-nitrophenyl)-N-(2-methoxybenzyl)-ethan-1-amine Hydrochloride (25N-NBOMe, **2f**).* Synthesized from 2-(2,5-dimethoxy-4-nitrophenyl)ethan-1-amine hydrochloride and 2-methoxybenzaldehyde by general procedure A in 73% yield as an orange solid. ^{1}H NMR (600 MHz, DMSO) δ 9.11 (s, 2H), 7.51 (s, 1H), 7.48 (dd, J = 7.5, 1.7 Hz, 1H), 7.42 (ddd, J = 8.3, 7.4, 1.7 Hz, 1H), 7.29 (s, 1H), 7.10 (dd, J = 8.3, 1.0 Hz, 1H), 7.01 (td, J = 7.4, 1.0 Hz, 1H), 4.14 (t, J = 5.4 Hz, 2H), 3.89 (s, 3H), 3.84 (s, 3H), 3.81 (s, 3H), 3.19−3.11 (m, 2H), 3.09−3.03 (m, 2H). ^{13}C NMR (151 MHz, DMSO) δ 157.5, 150.4, 146.1, 137.7, 132.4, 131.4, 130.8, 120.4, 119.6, 116.7, 111.1, 107.3, 57.0, 56.3, 55.6, 45.5, 45.0, 26.4.

*3.2.1.15. 2-(2,5-Dimethoxy-4-nitrophenyl)-N-(2-fluorobenzyl)-ethan-1-amine Hydrochloride (25N-NBF, **2g**).* Synthesized from 2-(2,5-dimethoxy-4-nitrophenyl)ethan-1-amine hydrochloride and 2-fluorobenzaldehyde by general procedure A in 69% yield as an orange solid. ^{1}H NMR (600 MHz, DMSO) δ 7.43 (t, J = 7.6 Hz, 1H), 7.28 (q, J = 6.3 Hz, 1H), 7.14 (m, J = 5.8, 1H), 3.86 (s, 3H), 3.79 (s, 3H), 3.76 (s, 2H), 2.79 (t, J = 6.2, 2H), 2.75 (t, J = 6.6 Hz, 2H). ^{13}C NMR (151 MHz, DMSO) δ 161.2, 150.3, 146.3, 136.8, 136.5, 130.3, 128.4, 124.1, 116.5, 114.9, 114.8, 107.0, 56.8, 56.1, 48.1, 45.6, 30.4.

*3.2.1.16. N-(Benzo[d][1,3]dioxol-4-ylmethyl)-2-(2,5-dimethoxy-4-nitrophenyl)ethan-1-amine Hydrochloride (25N-NBMD, **2h**).* Synthesized from 2-(2,5-dimethoxy-4-nitrophenyl)ethan-1-amine hydrochloride and 2,3-(methylenedioxy)benzaldehyde by general procedure A in 70% yield as an orange solid. ^{1}H NMR (400 MHz, DMSO) δ 7.44 (s, 1H), 7.21 (s, 1H), 6.83 (m, J = 3.3 Hz, 1H), 6.78 (m, J = 3.1 Hz, 2H), 5.96 (s, 2H), 3.85 (s, 3H), 3.78 (s, 3H), 3.67 (s, 2H), 2.76 (m, J = 5.3 Hz, 4H). ^{13}C NMR (151 MHz, DMSO) δ 150.5, 147.2, 146.2, 137.8, 132.4, 123.2, 121.9, 116.8, 113.1, 109.3, 107.4, 101.3, 57.1, 56.4, 45.6, 43.7, 26.6.

*3.2.1.17. 4-(2-Aminoethyl)-2,5-dimethoxybenzonitrile Hydrochloride (2C-CN, **1j**).* **1j** was prepared according to reported conditions, and the characterization was in accordance with reported values.[61]

3.3. NanoBiT Functional Complementation Assays.

Two functional complementation assays, employing the NanoBiT system to monitor the recruitment of either SmBiT-βarr2 or SmBiT-miniGα_q to 5-HT$_{2A}$-LgBiT, were carried out in parallel, as described before.[32,38] NanoBiT employs two subunits of a split nanoluciferase (SmBiT and LgBiT) to monitor protein-protein interactions in live cells. To this end, each interacting partner, here 5-HT$_{2A}$ and either βarr2 or miniGα_q, is fused to one of the enzyme fragments. Upon protein interaction, i.e., the recruitment of βarr2 or miniGα_q to the agonist-bound 5-HT$_{2A}$, the inactive subunits of the split nanoluciferase are functionally complemented, leading to a luminescent signal in the presence of the enzyme's substrate.[63] Transient transfection of HEK (Human Embryonic Kidney) 293T cells was used, as—for unknown reasons—previous attempts to establish a stable cell system co-expressing 5-HT$_{2A}$-LgBiT with SmBiT-miniGα_q were not successful (in contrast to the successful generation of a 5-HT$_{2A}$-LgBiT−SmBiT-βarr2 cell line).

More specifically, HEK293T cells were routinely cultured in DMEM supplemented with 10% heat-inactivated FBS, 100 IU/mL of penicillin, 100 μg/mL of streptomycin, and 0.25 μg/mL amphotericin B, at 37 °C and 5% CO_2 in a humidified atmosphere. For the assay, the cells were seeded in 6-well plates at a density of 500 000 cells per well, and incubated overnight. Subsequently, each well was transfected with 3.3 μg of DNA (consisting of 1.65 μg of 5-HT$_{2A}$-LgBiT construct and 1.65 μg of either SmBiT-βarr2 or SmBiT-miniGα_q), using FuGENE HD transfection reagent in a 3:1 FuGENE:DNA ratio in OptiMEM, according to the manufacturer's protocol. Twenty-four hours post-transfection, the cells were reseeded in poly-D-lysine coated 96-well plates at a density of 50 000 cells per well. Following overnight incubation, the cells were washed twice with HBSS, and 100 μL of HBSS was added to each well. To this, 25 μL of NanoGlo Live Cell reagent (diluted 1/20 in the provided LCS dilution buffer, according to the manufacturer's protocol), was added, and the plate was placed in the Tristar^2 LB 942 multimode microplate reader (Berthold Technologies GmbH & Co, Germany) until equilibration of the signal. After the equilibration phase, 10 μL of 13.5× concentrated agonist solutions were added, and the luminescent signal was continuously monitored for 2 h (resulting in each well being measured every 2 min) at room temperature. Each substance was measured in at least three independent experiments, with duplicates per concentration, and including a concentration range of reference agonists LSD and serotonin per experiment, along with the appropriate solvent controls.

3.3.1. Data Analysis. Data were analyzed as previously described in more detail.[64] The obtained time-luminescence profiles were corrected for inter-well variability, and the area under the curve (AUC) was calculated. After subtraction of the corresponding blank's AUC, the values were transferred to GraphPad Prism software (San Diego, CA). Concentration−response curves were fit through a three parametric nonlinear regression analysis (as a Hill slope of 1 is required for the calculation of the bias factors), followed by normalization of the data of the individual experiments, with the maximal response of the respective reference agonist defined as 100%. Subsequently, all normalized data from the individual experiments were pooled, and total EC$_{50}$ and E_{max} values were generated by fitting the curve through the normalized and pooled data of the individual concentration points. A schematic overview of this procedure is provided in Figure S1.

Bias plots were generated by means of a centered second-order polynomial fitting of the normalized and pooled data obtained for the individual concentration points in the βarr2 (abscissa) or miniGα_q (ordinate) assay format. Bias factors (β_i) were calculated following the relative intrinsic activity approach.[22,65] For each compound, RA$_i$ values were calculated respective to either reference agonist, and in each assay format separately

$$\mathrm{RA}_{i,\text{reference agonist}}^{\text{pathway}} = \frac{\frac{E_{max,i}}{EC_{50,i}}}{\frac{E_{max,reference}}{EC_{50,reference}}} = \frac{EC_{50,reference} \times E_{max,i}}{E_{max,reference} \times EC_{50,i}}$$

https://doi.org/10.1021/acschemneuro.3c00267
ACS Chem. Neurosci. 2023, 14, 2727−2742

Per individual compound, the RA_i values were then combined into a bias factor, β_i, for the respective reference agonist (either LSD or serotonin)

$$\beta_i = \log\left(\frac{RA_{i,reference}^{\beta arr2}}{RA_{i,reference}^{miniG\alpha_q}}\right)$$

The formula implies that the reference agonist used will have a β_i of 0, whereas a compound with a positive value for β_i preferentially induced the recruitment of βarr2 over the recruitment of miniGα_q, compared to the respective reference agonist, and vice versa. A Kruskal–Wallis analysis (the nonparametric alternative to one-way ANOVA) with post hoc Dunn's test was used to estimate the statistical probability of a certain β_i to be different from 0.

3.4. Molecular Modeling. All molecular modeling calculations were performed in the Schrödinger Drug Discovery Suite (Release 2021-4, Schrödinger LLC, New York, NY, 2021). The ligands were sketched in Maestro (2D Sketcher). Charges, ionization states at pH 7.0 ± 2.0, 3D coordinates, and conformational minimization were performed with LigPrep in default settings and the OPLS4 force field.[66] For the ligands with multiple protonation states, only the state with a positive charge on the amine was kept, as the salt-bridge interaction between this group and Asp155^{3x32} is recognized as critical for ligand binding.[67] For DOX (DOT, DOT-7), only the *R*-isomers were selected for docking, as these are the most active.[68]

The cryo-EM structure of the 5-HT_{2A} in complex to 25CN-NBOH and bound to a miniGα_q protein chimera[54] was downloaded from PDB (accession code 6WHA) and prepared in the Protein Preparation Wizard[69] using default settings. For 25CN-NBOH, the protonation states at pH 7.0 ± 2.0 were generated with Epik v5.8,[70,71] and the protonation state with a positive charge in the amine group was selected. The protein hydrogen bond network was optimized with ProPKA[72,73] at pH 7.0 and using ProtAssign[69] for the automatic optimization of hydroxyl, Asn, Gln, and His side chains. This was followed by two cycles of restrained minimization using Impact v9.3[74] in the OPLS4 force field with heavy atom convergence RMSD of 0.30 Å at each cycle. The prepared 5-HT_{2A} structure was used for docking grid generation. The docking grid was centered around the experimental ligand (25CN-NBOH), and no scaling factor was applied to the receptor atoms. The side chains of Ser159^{3x36}, Thr160^{3x37}, Ser239^{5x44}, Ser242^{5x461}, and Tyr370^{7x42} were defined with rotatable hydroxy groups. No additional constraints were applied, and all other settings were kept at default values.

Ligand dockings were performed in Glide v9.3[75,76] in extra precision mode[77] and the OPLS4 force field. The van der Waals radii of ligand atoms were not scaled, i.e., the default scaling value was changed from 0.8 to 1.0, as the docking involved a congeneric series to the experimental ligand. The sampling of nitrogen inversions and ring conformations were allowed, as well as enhanced planarity for conjugated π groups. Five docking poses were written per ligand, followed by a post-docking optimization with a rejection threshold of 0.50 kcal/mol and the application of strain correction terms. All other settings were kept in the standard (default) values. The docking poses were selected based on the lowest docking score and lowest RMSD to the experimentally bound ligand.

Ligand–receptor interaction and structural interaction fingerprints (SIFt) were calculated and visualized using PyMOL (The PyMOL Molecular Graphics System, Schrödinger LLC, New York, 2020) and using the plugin Intermezzo (v1.2, Ochoa et al., unpublished, available at http://mordred.bioc.cam.ac.uk/intermezzo). The pocket was defined by a set of residues within 5.0 Å of 25CN-NBOH in the template structure. The distribution constant between octanol/water at pH 7.40 ($c\log D_{7.4}$) was calculated in Chemicalize (ChemAxon Kft., Budapest, 2022). Linear correlation curves and other statistical analysis methods were done in OriginPro 2020 (OriginLab Corporation, Northampton, 2019), which was also used to generate the plots. The statistical significance of correlations was assessed via analysis of covariance (ANOVA) with a confidence level of 95%. The GPCRdb numbering scheme was used to assign the generic residue numbers throughout the manuscript and figures.[78]

■ ASSOCIATED CONTENT

Supporting Information

The Supporting Information is available free of charge at https://pubs.acs.org/doi/10.1021/acschemneuro.3c00267.

Schematic overview of data analysis; assessment of relative 5-HT_{2A}-LgBiT expression in (non-) serum-starved cells; comparison of assay results in cells cultured in medium containing no serum (serum-starved), dialyzed serum, or "normal" fetal bovine serum; comparison between experimental and docked binding pose of 25CN-NBOH; estimated distances between the docked binding pose of the phenethylamines and the residues lining the hydrophobic pocket between TM4 and TM5; quantification of the results with the 30 min AUC (area under the curve) values and LSD as a reference agonist; quantification of the results with serotonin as the reference agonist; and quantification of the results with the 30 min AUC (area under the curve) values and serotonin as a reference agonist (PDF)

■ AUTHOR INFORMATION

Corresponding Authors

Jesper L. Kristensen − *Department of Drug Design and Pharmacology, Faculty of Health and Medical Sciences, University of Copenhagen, DK-2100 Copenhagen, Denmark;* orcid.org/0000-0002-5613-1267; Phone: +45 35 33 64 87; Email: jesper.kristensen@sund.ku.dk

Christophe P. Stove − *Laboratory of Toxicology, Department of Bioanalysis, Faculty of Pharmaceutical Sciences, Ghent University, B-9000 Ghent, Belgium;* orcid.org/0000-0001-7126-348X; Phone: +32 9 264 81 35; Email: christophe.stove@ugent.be; Fax: +32 9 264 81 83

Authors

Eline Pottie − *Laboratory of Toxicology, Department of Bioanalysis, Faculty of Pharmaceutical Sciences, Ghent University, B-9000 Ghent, Belgium*

Christian B. M. Poulie − *Department of Drug Design and Pharmacology, Faculty of Health and Medical Sciences, University of Copenhagen, DK-2100 Copenhagen, Denmark;* orcid.org/0000-0003-2662-9803

Icaro A. Simon − *Department of Drug Design and Pharmacology, Faculty of Health and Medical Sciences, University of Copenhagen, DK-2100 Copenhagen, Denmark;* orcid.org/0000-0003-4550-4248

Kasper Harpsøe − *Department of Drug Design and Pharmacology, Faculty of Health and Medical Sciences, University of Copenhagen, DK-2100 Copenhagen, Denmark;* orcid.org/0000-0002-9326-9644

Laura D'Andrea − *Department of Drug Design and Pharmacology, Faculty of Health and Medical Sciences, University of Copenhagen, DK-2100 Copenhagen, Denmark*

Igor V. Komarov − *Enamine Ltd., Kyiv 02094, Ukraine;* orcid.org/0000-0002-7908-9145

David E. Gloriam − *Department of Drug Design and Pharmacology, Faculty of Health and Medical Sciences, University of Copenhagen, DK-2100 Copenhagen, Denmark;* orcid.org/0000-0002-4299-7561

https://doi.org/10.1021/acschemneuro.3c00267
ACS Chem. Neurosci. 2023, 14, 2727−2742

Anders A. Jensen − *Department of Drug Design and Pharmacology, Faculty of Health and Medical Sciences, University of Copenhagen, DK-2100 Copenhagen, Denmark*

Complete contact information is available at: https://pubs.acs.org/10.1021/acschemneuro.3c00267

Author Contributions

‖E.P. and C.B.M.P. contributed equally to this manuscript. Conceptualization: E.P., C.B.M.P., I.A.S., A.A.J., J.L.K., C.P.S. Experiments and formal analysis: E.P., C.B.M.P., I.A.S., L.D. Writing—original draft: E.P., C.B.M.P., I.A.S. Writing—review and editing: K.H., L.D., I.V.K., D.E.G., A.A.J., J.L.K., C.P.S.

Notes

The authors declare the following competing financial interest(s): D.E.G. is a part-time employee and warrant holder of Kvantify.

■ ACKNOWLEDGMENTS

Gemma De Baere is acknowledged for practical assistance during the experiments. This project has received funding from the European Union's Horizon 2020 Research and Innovation Program under the Marie Sklodowska−Curie Grant Agreement No. 765657. D.E.G. acknowledges financial support from the Novo Nordisk Foundation (NNF18OC0031226) and the Lundbeck Foundation (R313-2019-526). I.A.S. and L.D. acknowledge the EU Horizon 2020, Innovative Training Network SAFER (765657).

■ REFERENCES

(1) Barnes, N. M.; Ahern, G. P.; Becamel, C.; Bockaert, J.; Camilleri, M.; Chaumont-Dubel, S.; Claeysen, S.; Cunningham, K. A.; Fone, K. C.; Gershon, M.; et al. International Union of Basic and Clinical Pharmacology. CX. Classification of Receptors for 5-hydroxytryptamine; Pharmacology and Function. *Pharmacol. Rev.* **2021**, *73*, 310−520.

(2) Nichols, D. E. Hallucinogens. *Pharmacol. Ther.* **2004**, *101*, 131−181.

(3) Glennon, R. A.; Titeler, M.; McKenney, J. D. Evidence for 5-HT2 involvement in the mechanism of action of hallucinogenic agents. *Life Sci.* **1984**, *35*, 2505−2511.

(4) Halberstadt, A. L. Recent advances in the neuropsychopharmacology of serotonergic hallucinogens. *Behav. Brain Res.* **2015**, *277*, 99−120.

(5) McClure-Begley, T. D.; Roth, B. L. The promises and perils of psychedelic pharmacology for psychiatry. *Nat. Rev. Drug Discovery* **2022**, *21*, 463−473.

(6) Nichols, D. E. Chemistry and Structure-Activity Relationships of Psychedelics. *Curr. Top. Behav. Neurosci.* **2018**, *36*, 1−43.

(7) Shulgin, A.; Shulgin, A. *PiHKAL: A Chemical Love Story* Transform Press, 1991.

(8) Shulgin, A.; Shulgin, A.*TiHKAL: The Continuation*; Transform Press, 1997.

(9) Poulie, C. B. M.; Jensen, A. A.; Halberstadt, A. L.; Kristensen, J. L. DARK Classics in Chemical Neuroscience: NBOMes. *ACS Chem. Neurosci.* **2020**, *11*, 3860−3869.

(10) Luethi, D.; Liechti, M. E. Designer drugs: mechanism of action and adverse effects. *Arch. Toxicol.* **2020**, *94*, 1085−1133.

(11) Nichols, D. E. Psychedelics. *Pharmacol. Rev.* **2016**, *68*, 264−355.

(12) Bogenschutz, M. P.; Ross, S. Therapeutic Applications of Classic Hallucinogens. *Curr. Top. Behav. Neurosci.* **2018**, *36*, 361−391.

(13) Kozlowska, U.; Nichols, C.; Wiatr, K.; Figiel, M. From psychiatry to neurology: Psychedelics as prospective therapeutics for neurodegenerative disorders. *J. Neurochem.* **2022**, *162*, 89−108.

(14) Avet, C.; Mancini, A.; Breton, B.; Le Gouill, C.; Hauser, A. S.; Normand, C.; Kobayashi, H.; Gross, F.; Hogue, M.; Lukasheva, V.; et al. Effector membrane translocation biosensors reveal G protein and betaarrestin coupling profiles of 100 therapeutically relevant GPCRs. *eLife* **2022**, *11*, No. e74101.

(15) Inoue, A.; Raimondi, F.; Kadji, F. M. N.; Singh, G.; Kishi, T.; Uwamizu, A.; Ono, Y.; Shinjo, Y.; Ishida, S.; Arang, N.; et al. Illuminating G-Protein-Coupling Selectivity of GPCRs. *Cell* **2019**, *177*, 1933−1947.

(16) Vargas, M. V.; Dunlap, L. E.; Dong, C.; Carter, S. J.; Tombari, R. J.; Jami, S. A.; Cameron, L. P.; Patel, S. D.; Hennessey, J. J.; Saeger, H. N.; et al. Psychedelics promote neuroplasticity through the activation of intracellular 5-HT2A receptors. *Science* **2023**, *379*, 700−706.

(17) Cunningham, M. J.; Bock, H. A.; Serrano, I. C.; Bechand, B.; Vidyadhara, D. J.; Bonniwell, E. M.; Lankri, D.; Duggan, P.; Nazarova, A. L.; Cao, A. B.; et al. Pharmacological Mechanism of the Non-hallucinogenic 5-HT(2A) Agonist Ariadne and Analogs. *ACS Chem. Neurosci.* **2023**, *14*, 119−135.

(18) Kolb, P.; Kenakin, T.; Alexander, S. P. H.; Bermudez, M.; Bohn, L. M.; Breinholt, C. S.; Bouvier, M.; Hill, S. J.; Kostenis, E.; Martemyanov, K.; et al. Community Guidelines for GPCR Ligand Bias: IUPHAR Review XX. *Br. J. Pharmacol.* **2022**, *179*, 3651−3674.

(19) López-Giménez, J. F.; Gonzalez-Maeso, J. Hallucinogens and Serotonin 5-HT2A Receptor-Mediated Signaling Pathways. *Curr. Top. Behav. Neurosci.* **2018**, *36*, 45−73.

(20) Onaran, H. O.; Ambrosio, C.; Ugur, O.; Madaras Koncz, E.; Gro, M. C.; Vezzi, V.; Rajagopal, S.; Costa, T. Systematic errors in detecting biased agonism: Analysis of current methods and development of a new model-free approach. *Sci. Rep.* **2017**, *7*, No. 44247.

(21) Nagi, K.; Pineyro, G. Practical guide for calculating and representing biased signaling by GPCR ligands: A stepwise approach. *Methods* **2016**, *92*, 78−86.

(22) Rajagopal, S.; Ahn, S.; Rominger, D. H.; Gowen-MacDonald, W.; Lam, C. M.; Dewire, S. M.; Violin, J. D.; Lefkowitz, R. J. Quantifying ligand bias at seven-transmembrane receptors. *Mol. Pharmacol.* **2011**, *80*, 367−377.

(23) Kenakin, T. Biased Receptor Signaling in Drug Discovery. *Pharmacol. Rev.* **2019**, *71*, 267−315.

(24) Berg, K. A.; Maayani, S.; Goldfarb, J.; Scaramellini, C.; Leff, P.; Clarke, W. P. Effector pathway-dependent relative efficacy at serotonin type 2A and 2C receptors: evidence for agonist-directed trafficking of receptor stimulus. *Mol. Pharmacol.* **1998**, *54*, 94−104.

(25) Roth, B. L.; Chuang, D. M. Multiple mechanisms of serotonergic signal transduction. *Life Sci.* **1987**, *41*, 1051−1064.

(26) Kurrasch-Orbaugh, D. M.; Watts, V. J.; Barker, E. L.; Nichols, D. E. Serotonin 5-hydroxytryptamine 2A receptor-coupled phospholipase C and phospholipase A2 signaling pathways have different receptor reserves. *J. Pharmacol. Exp. Ther.* **2003**, *304*, 229−237.

(27) McLean, T. H.; Parrish, J. C.; Braden, M. R.; Marona-Lewicka, D.; Gallardo-Godoy, A.; Nichols, D. E. 1-Aminomethylbenzocycloalkanes: conformationally restricted hallucinogenic phenethylamine analogues as functionally selective 5-HT2A receptor agonists. *J. Med. Chem.* **2006**, *49*, 5794−5803.

(28) Moya, P. R.; Berg, K. A.; Gutierrez-Hernandez, M. A.; Saez-Briones, P.; Reyes-Parada, M.; Cassels, B. K.; Clarke, W. P. Functional selectivity of hallucinogenic phenethylamine and phenylisopropylamine derivatives at human 5-hydroxytryptamine (5-HT)2A and 5-HT2C receptors. *J. Pharmacol. Exp. Ther.* **2007**, *321*, 1054−1061.

(29) Martí-Solano, M.; Iglesias, A.; de Fabritiis, G.; Sanz, F.; Brea, J.; Loza, M. I.; Pastor, M.; Selent, J. Detection of new biased agonists for the serotonin 5-HT2A receptor: modeling and experimental validation. *Mol. Pharmacol.* **2015**, *87*, 740−746.

(30) Wacker, D.; Wang, S.; McCorvy, J. D.; Betz, R. M.; Venkatakrishnan, A. J.; Levit, A.; Lansu, K.; Schools, Z. L.; Che, T.; Nichols, D. E.; et al. Crystal Structure of an LSD-Bound Human Serotonin Receptor. *Cell* **2017**, *168*, 377−389.

(31) Blough, B. E.; Landavazo, A.; Decker, A. M.; Partilla, J. S.; Baumann, M. H.; Rothman, R. B. Interaction of psychoactive

tryptamines with biogenic amine transporters and serotonin receptor subtypes. *Psychopharmacology* **2014**, *231*, 4135−4144.
(32) Pottie, E.; Dedecker, P.; Stove, C. P. Identification of psychedelic new psychoactive substances (NPS) showing biased agonism at the 5-HT2AR through simultaneous use of beta-arrestin 2 and miniGalphaq bioassays. *Biochem. Pharmacol.* **2020**, *182*, No. 114251.
(33) Cao, D.; Yu, J.; Wang, H.; Luo, Z.; Liu, X.; He, L.; Qi, J.; Fan, L.; Tang, L.; Chen, Z.; et al. Structure-based discovery of nonhallucinogenic psychedelic analogs. *Science* **2022**, *375*, 403−411.
(34) Poulie, C. B. M.; Pottie, E.; Simon, I. A.; Harpsoe, K.; D'Andrea, L.; Komarov, I. V.; Gloriam, D. E.; Jensen, A. A.; Stove, C. P.; Kristensen, J. L. Discovery of beta-Arrestin-Biased 25CN-NBOH-Derived 5-HT(2A) Receptor Agonists. *J. Med. Chem.* **2022**, *65*, 12031−12043.
(35) Kaplan, A. L.; Confair, D. N.; Kim, K.; Barros-Alvarez, X.; Rodriguiz, R. M.; Yang, Y.; Kweon, O. S.; Che, T.; McCorvy, J. D.; Kamber, D. N.; et al. Bespoke library docking for 5-HT(2A) receptor agonists with antidepressant activity. *Nature* **2022**, *610*, 582−591.
(36) Lane, J. R.; May, L. T.; Parton, R. G.; Sexton, P. M.; Christopoulos, A. A kinetic view of GPCR allostery and biased agonism. *Nat. Chem. Biol.* **2017**, *13*, 929−937.
(37) Pottie, E.; Stove, C. P. In vitro assays for the functional characterization of (psychedelic) substances at the serotonin receptor 5-HT2A R. *J. Neurochem.* **2022**, *162*, 39−59.
(38) Pottie, E.; Kupriyanova, O. V.; Brandt, A. L.; Laprairie, R. B.; Shevyrin, V. A.; Stove, C. P. Serotonin 2A Receptor (5-HT2AR) Activation by 25H-NBOMe Positional Isomers: In Vitro Functional Evaluation and Molecular Docking. *ACS Pharmacol. Transl. Sci.* **2021**, *4*, 479−487.
(39) Nehmé, R.; Carpenter, B.; Singhal, A.; Strege, A.; Edwards, P. C.; White, C. F.; Du, H.; Grisshammer, R.; Tate, C. G. Mini-G proteins: Novel tools for studying GPCRs in their active conformation. *PLoS One* **2017**, *12*, No. e0175642.
(40) Pottie, E.; Cannaert, A.; Van Uytfanghe, K.; Stove, C. P. Setup of a Serotonin 2A Receptor (5-HT2AR) Bioassay: Demonstration of Its Applicability To Functionally Characterize Hallucinogenic New Psychoactive Substances and an Explanation Why 5-HT2AR Bioassays Are Not Suited for Universal Activity-Based Screening of Biofluids for New Psychoactive Substances. *Anal. Chem.* **2019**, *91*, 15444−15452.
(41) Pottie, E.; Cannaert, A.; Stove, C. P. In vitro structure-activity relationship determination of 30 psychedelic new psychoactive substances by means of beta-arrestin 2 recruitment to the serotonin 2A receptor. *Arch. Toxicol.* **2020**, *94*, 3449−3460.
(42) Pottie, E.; Kupriyanova, O. V.; Shevyrin, V. A.; Stove, C. P. Synthesis and Functional Characterization of 2-(2,5-Dimethoxyphenyl)-N-(2-fluorobenzyl)ethanamine (25H-NBF) Positional Isomers. *ACS Chem. Neurosci.* **2021**, *12*, 1667−1673.
(43) Swain, M. chemicalize.org. *J. Chem. Inf. Model.* **2012**, *52*, 613−615.
(44) Parrish, J. C.; Braden, M. R.; Gundy, E.; Nichols, D. E. Differential phospholipase C activation by phenylalkylamine serotonin 5-HT 2A receptor agonists. *J. Neurochem.* **2005**, *95*, 1575−1584.
(45) Braden, M. R.; Parrish, J. C.; Naylor, J. C.; Nichols, D. E. Molecular interaction of serotonin 5-HT2A receptor residues Phe339(6.51) and Phe340(6.52) with superpotent N-benzyl phenethylamine agonists. *Mol. Pharmacol.* **2006**, *70*, 1956−1964.
(46) Rickli, A.; Luethi, D.; Reinisch, J.; Buchy, D.; Hoener, M. C.; Liechti, M. E. Receptor interaction profiles of novel N-2-methoxybenzyl (NBOMe) derivatives of 2,5-dimethoxy-substituted phenethylamines (2C drugs). *Neuropharmacology* **2015**, *99*, 546−553.
(47) Eshleman, A. J.; Wolfrum, K. M.; Reed, J. F.; Kim, S. O.; Johnson, R. A.; Janowsky, A. Neurochemical pharmacology of psychoactive substituted N-benzylphenethylamines: High potency agonists at 5-HT2A receptors. *Biochem. Pharmacol.* **2018**, *158*, 27−34.
(48) Hansen, M.; Phonekeo, K.; Paine, J. S.; Leth-Petersen, S.; Begtrup, M.; Brauner-Osborne, H.; Kristensen, J. L. Synthesis and structure-activity relationships of N-benzyl phenethylamines as 5-HT2A/2C agonists. *ACS Chem. Neurosci.* **2014**, *5*, 243−249.
(49) Jensen, A. A.; McCorvy, J. D.; Leth-Petersen, S.; Bundgaard, C.; Liebscher, G.; Kenakin, T. P.; Brauner-Osborne, H.; Kehler, J.; Kristensen, J. L. Detailed Characterization of the In Vitro Pharmacological and Pharmacokinetic Properties of N-(2-Hydroxybenzyl)-2,5-Dimethoxy-4-Cyanophenylethylamine (25CN-NBOH), a Highly Selective and Brain-Penetrant 5-HT2A Receptor Agonist. *Pharmacol. Exp. Ther.* **2017**, *361*, 441−453.
(50) Jensen, A. A.; Halberstadt, A. L.; Marcher-Rorsted, E.; Odland, A. U.; Chatha, M.; Speth, N.; Liebscher, G.; Hansen, M.; Brauner-Osborne, H.; Palner, M.; et al. The selective 5-HT2A receptor agonist 25CN-NBOH: Structure-activity relationship, in vivo pharmacology, and in vitro and ex vivo binding characteristics of [(3)H]25CN-NBOH. *Biochem. Pharmacol.* **2020**, *177*, No. 113979.
(51) Nichols, D. E.; Dyer, D. C. Lipophilicity and serotonin agonist activity in a series of 4-substituted mescaline analogues. *J. Med. Chem.* **1977**, *20*, 299−301.
(52) Seggel, M. R.; Yousif, M. Y.; Lyon, R. A.; Titeler, M.; Roth, B. L.; Suba, E. A.; Glennon, R. A. A structure-affinity study of the binding of 4-substituted analogues of 1-(2,5-dimethoxyphenyl)-2-aminopropane at 5-HT2 serotonin receptors. *J. Med. Chem.* **1990**, *33*, 1032−1036.
(53) Parker, M. A.; Kurrasch, D. M.; Nichols, D. E. The role of lipophilicity in determining binding affinity and functional activity for 5-HT2A receptor ligands. *Bioorg. Med. Chem.* **2008**, *16*, 4661−4669.
(54) Kim, K.; Che, T.; Panova, O.; DiBerto, J. F.; Lyu, J.; Krumm, B. E.; Wacker, D.; Robertson, M. J.; Seven, A. B.; Nichols, D. E.; et al. Structure of a Hallucinogen-Activated Gq-Coupled 5-HT2A Serotonin Receptor. *Cell* **2020**, *182*, 1574−1588.
(55) Vass, M.; Podlewska, S.; de Esch, I. J. P.; Bojarski, A. J.; Leurs, R.; Kooistra, A. J.; de Graaf, C. Aminergic GPCR-Ligand Interactions: A Chemical and Structural Map of Receptor Mutation Data. *J. Med. Chem.* **2019**, *62*, 3784−3839.
(56) Choudhary, M. S.; Craigo, S.; Roth, B. L. A single point mutation (Phe340−>Leu340) of a conserved phenylalanine abolishes 4-[125I]iodo-(2,5-dimethoxy)phenylisopropylamine and [3H]-mesulergine but not [3H]ketanserin binding to 5-hydroxytryptamine2 receptors. *Mol. Pharmacol.* **1993**, *43*, 755−761.
(57) Xu, P.; Huang, S.; Zhang, H.; Mao, C.; Zhou, X. E.; Cheng, X.; Simon, I. A.; Shen, D. D.; Yen, H. Y.; Robinson, C. V.; et al. Structural insights into the lipid and ligand regulation of serotonin receptors. *Nature* **2021**, *592*, 469−473.
(58) Eisenberg, D.; Schwarz, E.; Komaromy, M.; Wall, R. Analysis of membrane and surface protein sequences with the hydrophobic moment plot. *J. Mol. Biol.* **1984**, *179*, 125−142.
(59) Gregory, K. J.; Hall, N. E.; Tobin, A. B.; Sexton, P. M.; Christopoulos, A. Identification of orthosteric and allosteric site mutations in M2 muscarinic acetylcholine receptors that contribute to ligand-selective signaling bias. *J. Biol. Chem.* **2010**, *285*, 7459−7474.
(60) Leth-Petersen, S.; Petersen, I. N.; Jensen, A. A.; Bundgaard, C.; Baek, M.; Kehler, J.; Kristensen, J. L. 5-HT2A/5-HT2C Receptor Pharmacology and Intrinsic Clearance of N-Benzylphenethylamines Modified at the Primary Site of Metabolism. *ACS Chem. Neurosci.* **2016**, *7*, 1614−1619.
(61) Cheng, A. C.; Castagnoli, N., Jr. Synthesis and physicochemical and neurotoxicity studies of 1-(4-substituted-2,5-dihydroxyphenyl)-2-aminoethane analogues of 6-hydroxydopamine. *J. Med. Chem.* **1984**, *27*, 513−520.
(62) Gallardo-Godoy, A.; Fierro, A.; McLean, T. H.; Castillo, M.; Cassels, B. K.; Reyes-Parada, M.; Nichols, D. E. Sulfur-substituted alpha-alkyl phenethylamines as selective and reversible MAO-A inhibitors: biological activities, CoMFA analysis, and active site modeling. *J. Med. Chem.* **2005**, *48*, 2407−2419.
(63) Dixon, A. S.; Schwinn, M. K.; Hall, M. P.; Zimmerman, K.; Otto, P.; Lubben, T. H.; Butler, B. L.; Binkowski, B. F.; Machleidt, T.; Kirkland, T. A.; et al. NanoLuc Complementation Reporter Optimized for Accurate Measurement of Protein Interactions in Cells. *ACS Chem. Biol.* **2016**, *11*, 400−408.

https://doi.org/10.1021/acschemneuro.3c00267
ACS Chem. Neurosci. 2023, 14, 2727−2742

(64) Pottie, E.; Tosh, D. K.; Gao, Z. G.; Jacobson, K. A.; Stove, C. P. Assessment of Biased Agonism at the A3 Adenosine Receptor using Beta-arrestin and MiniGalphai Recruitment Assays. *Biochem. Pharmacol.* **2020**, *177*, No. 113934.
(65) Ehlert, F. J. On the analysis of ligand-directed signaling at G protein-coupled receptors. *Naunyn-Schmiedeberg's Arch. Pharmacol.* **2008**, *377*, 549−577.
(66) Lu, C.; Wu, C.; Ghoreishi, D.; Chen, W.; Wang, L.; Damm, W.; Ross, G. A.; Dahlgren, M. K.; Russell, E.; Von Bargen, C. D.; et al. OPLS4: Improving Force Field Accuracy on Challenging Regimes of Chemical Space. *J. Chem. Theory Comput.* **2021**, *17*, 4291−4300.
(67) Almaula, N.; Ebersole, B. J.; Zhang, D.; Weinstein, H.; Sealfon, S. C. Mapping the binding site pocket of the serotonin 5-Hydroxytryptamine2A receptor. Ser3.36(159) provides a second interaction site for the protonated amine of serotonin but not of lysergic acid diethylamide or bufotenin. *J. Biol. Chem.* **1996**, *271*, 14672−14675.
(68) Nichols, D. E. Structure-activity relationships of serotonin 5-HT_{2A} agonists. *WIREs Membr. Transp. Signal.* **2012**, *1*, 559−579.
(69) Madhavi Sastry, G.; Adzhigirey, M.; Day, T.; Annabhimoju, R.; Sherman, W. Protein and ligand preparation: parameters, protocols, and influence on virtual screening enrichments. *J. Comput.-Aided Mol. Des.* **2013**, *27*, 221−234.
(70) Shelley, J. C.; Cholleti, A.; Frye, L. L.; Greenwood, J. R.; Timlin, M. R.; Uchimaya, M. Epik: a software program for pK(a) prediction and protonation state generation for drug-like molecules. *J. Comput.-Aided Mol. Des.* **2007**, *21*, 681−691.
(71) Greenwood, J. R.; Calkins, D.; Sullivan, A. P.; Shelley, J. C. Towards the comprehensive, rapid, and accurate prediction of the favorable tautomeric states of drug-like molecules in aqueous solution. *J. Comput.-Aided Mol. Des.* **2010**, *24*, 591−604.
(72) Søndergaard, C. R.; Olsson, M. H.; Rostkowski, M.; Jensen, J. H. Improved Treatment of Ligands and Coupling Effects in Empirical Calculation and Rationalization of pKa Values. *J. Chem. Theory Comput.* **2011**, *7*, 2284−2295.
(73) Olsson, M. H. M.; Sondergaard, C. R.; Rostkowski, M.; Jensen, J. H. PROPKA3: Consistent Treatment of Internal and Surface Residues in Empirical pKa Predictions. *J. Chem. Theory Comput.* **2011**, *7*, 525−537.
(74) Banks, J. L.; Beard, H. S.; Cao, Y.; Cho, A. E.; Damm, W.; Farid, R.; Felts, A. K.; Halgren, T. A.; Mainz, D. T.; Maple, J. R.; et al. Integrated Modeling Program, Applied Chemical Theory (IMPACT). *J. Comput. Chem.* **2005**, *26*, 1752−1780.
(75) Halgren, T. A.; Murphy, R. B.; Friesner, R. A.; Beard, H. S.; Frye, L. L.; Pollard, W. T.; Banks, J. L. Glide: a new approach for rapid, accurate docking and scoring. 2. Enrichment factors in database screening. *J. Med. Chem.* **2004**, *47*, 1750−1759.
(76) Friesner, R. A.; Banks, J. L.; Murphy, R. B.; Halgren, T. A.; Klicic, J. J.; Mainz, D. T.; Repasky, M. P.; Knoll, E. H.; Shelley, M.; Perry, J. K.; et al. Glide: a new approach for rapid, accurate docking and scoring. 1. Method and assessment of docking accuracy. *J. Med. Chem.* **2004**, *47*, 1739−1749.
(77) Friesner, R. A.; Murphy, R. B.; Repasky, M. P.; Frye, L. L.; Greenwood, J. R.; Halgren, T. A.; Sanschagrin, P. C.; Mainz, D. T. Extra precision glide: docking and scoring incorporating a model of hydrophobic enclosure for protein-ligand complexes. *J. Med. Chem.* **2006**, *49*, 6177−6196.
(78) Isberg, V.; de Graaf, C.; Bortolato, A.; Cherezov, V.; Katritch, V.; Marshall, F. H.; Mordalski, S.; Pin, J. P.; Stevens, R. C.; Vriend, G.; Gloriam, D. E. Generic GPCR residue numbers - aligning topology maps while minding the gaps. *Trends Pharmacol. Sci.* **2015**, *36*, 22−31.

https://doi.org/10.1021/acschemneuro.3c00267
ACS Chem. Neurosci. 2023, 14, 2727−2742